https://doi.org/10.5194/hess-2023-304
Preprint. Discussion started: 30 April 2024
© Author(s) 2024. CC BY 4.0 License.

Hydrology and Earth System Sciences
Open Access
Discussions

Implementation of global soil databases in NOAH-MP model and the effects on simulated mean and extreme soil hydrothermal changes

Kazeem A. Ishola[1,3] Gerald Mills[2], Ankur P. Sati[2], Benjamin Obe[2], Matthias Demuzere[5], Deepak Upreti[1,3], Gourav Misra[3], Paul Lewis[3], Daire Walsh[3], Tim McCarthy[3], Rowan Fealy[4,*]

[1]Irish Climate Analysis and Research UnitS (ICARUS), Maynooth University, Maynooth, Ireland
[2]School of Geography, University College Dublin, Dublin, Ireland
[3]National Centre for Geocomputation, Maynooth University, Maynooth, Ireland
[4]Department of Geography, Maynooth University, Maynooth, Ireland.
[5]B-Kode VOF, Ghent, Belgium
Correspondence to: Kazeem Ishola (Kazeem.Ishola@mu.ie) and Rowan Fealy (Rowan.Fealy@mu.ie)

Abstract

Soil properties and their associated hydro-physical parameters represent a significant source of uncertainty in Land Surface Models (LSMs) with consequent effects on simulated sub-surface thermal and moisture characteristics, surface energy exchanges and turbulent fluxes. These effects can result in large model differences particularly during extreme events. Typical of many model based approaches, spatial soil information such as location, extent and depth of textural classes are derived from coarse scale soil information and employed largely due to their ready availability rather than suitability. However, the use of a particular spatial soil dataset has important consequences for many of the processes simulated within a LSM. This study investigates NOAH-MP model uncertainty in simulating soil moisture (expressed as a ratio of water to soil volume, $m^3\ m^{-3}$) and soil temperature changes associated with two widely used global soil databases (STATSGO and SOILGRIDS) across the Island of Ireland. Both soil datasets produced a significant dry bias in loam soils, up to 0.15 $m^3\ m^{-3}$ in a wet period and 0.10 $m^3\ m^{-3}$ in a dry period. The spatial disparities between STATSGO and SOILGRIDS also influenced the regional soil hydrothermal changes and extremes. SOILGRIDS was found to intensify drought characteristics - shifting low/moderate drought areas into extreme/exceptional during dry periods - relative to STATSGO. Our results demonstrate that the coarse STATSGO performs as good as the fine-scale SOILGRIDS soil database. However, the results underscore the need to develop detailed regionally-derived soil texture characteristics, and for better representations of soil physics in LSMs to improve operational modeling and forecasting of hydrological processes and extremes.

Keywords: soil moisture; soil temperature, droughts; Land surface model; soil hydrophysical properties

https://doi.org/10.5194/hess-2023-304
Preprint. Discussion started: 30 April 2024
© Author(s) 2024. CC BY 4.0 License.

Hydrology and Earth System Sciences
Discussions

1. Introduction

The pedosphere (or soil) is an important component of the Earth system and plays a critical role in energy, water and biogeochemical exchanges that occur at the land-atmosphere interface (Dai et al., 2019a;b). The accurate description and representation of soil textural categories and/or soil hydro-physical properties is fundamental to developing and enhancing Earth system modeling (ESM) capacity in predicting land surface exchanges at different scales (Luo et al., 2016; Dai et al., 2019a,b). This information is incorporated via the respective land surface model (LSM) – the only physical boundary in an ESM and is a key component of any ESM framework (Fisher and Koven, 2020; Blyth et al., 2021). However, accurate descriptions of soil properties in LSMs are difficult to obtain due to the limited availability of high resolution global-scale soil texture measurements or lack of regionally specific measured soil properties (e.g. Kishné et al. 2017; Dennis and Berbery, 2021; 2022). This represents a key limitation and is a source of model uncertainty in current LSMs (Li et al., 2018), and consequently weather and climate models.

In many LSMs, soil hydrothermal properties such as saturated soil hydraulic conductivity and diffusivity, porosity, field capacity, wilting point, saturated soil matric potential, etc. are linked to soil textural classes/compositions in two ways. Typically, models employ a model-prescribed look-up table, with values that are empirically derived from existing/available in-situ soil surveys, to associate mean soil properties with each soil type. The soil categories are identified by grouping soil samples with similar properties using particle size analysis (e.g. Gee and Bauder, 2018). While this option is computational efficient, it assumes that the derived values are globally transferable which may not be realistic as soil properties vary both horizontally and vertically. This approach is also dependent on having access to soil texture maps; the scale and extent of which varies between different soil databases (Dai et al., 2019a,b; Dennis and Berbery, 2022). In spite of this, the use of readily available global soil texture maps in combination with model look-up tables is a standard practice in ESM research. As an alternative approach, new state-of-the-art global soil information datasets are being explored to constrain and improve the representation of soil processes within LSMs (e.g. de Lannoy et al., 2014; Shangguan et al., 2014; Hengl et al., 2017; Looy et al., 2017; Dennis and Berbery, 2021;2022; Xu et al., 2023). For some LSMs, soil hydrothermal properties can be estimated from a set of equations known as PedoTransfer Functions (PTFs) that require information on soil composition such as sand, silt and clay composition and organic matter (Looy et al., 2017; Dai et al., 2019a,b).

https://doi.org/10.5194/hess-2023-304
Preprint. Discussion started: 30 April 2024
© Author(s) 2024. CC BY 4.0 License.

The existing PTFs are based on different approaches (Looy et al., 2017) including, physically-based relationships or advanced statistical approaches based on machine learning, random forest and neural networks (Lehmann et al., 2018; Zhang et al., 2018; Or and Lehmann, 2019; Szabó et al. 2019). Clearly, the existing PTFs vary in complexity. Thus, the choice of PTFs partly depends on the availability of inputs (Weihermüller et al. 2021) and has been reported to impact soil moisture simulations, with consequent effects on the surface energy and water fluxes, land-atmosphere coupling, atmospheric moisture budget, boundary layer evolution and regional climate (Dennis and Berbery, 2021; 2022; Weihermüller et al. 2021; Xu et al., 2023; Zhang et al., 2023). Moreover, as soil moisture affects land-atmosphere interactions largely through its control on the evaporative fraction (e.g. Seneviratne et al., 2010; Ishola et al., 2022), soil hydrophysical properties play an important role in simulating climate extremes (e.g. droughts) (He et al., 2023; Zhang et al., 2023). Weihermüller et al. (2021), using the HYDRUS-1D model, reported that soil hydraulic properties estimated from different PTFs resulted in substantial variability in the predicted water fluxes. In this context, Dennis and Berbery (2021) and Dennis and Berbery (2022) employed soil properties derived from two different sources, the STATSGO and the Global Soil Dataset for Earth System Modelling (GSDE), in the Weather and Research Forecasting (WRF) and Community Land Model (CLM) models, and found soil texture-related differences in the surface fluxes that can lead to differences in the evolution of boundary layer thermodynamic structure and precipitation development. This finding is further supported by Zhang et al. (2023). Recently, Xu et al. (2023) demonstrated that using state-of-the-art soil information, such as POLARIS and the 250 m SoilGrids, can improve the performance of LSMs.

Here we focus on the response of the NOAH-MP LSM to soil information with the objectives evaluating the model representation of land surface fields; however, a LSM will also respond to changes in other drivers, such as vegetation (e.g. albedo, surface roughness length, etc.) and meteorological forcing (Arsenault et al., 2018; Hosseini et al., 2022). The first effort to implement SoilGrids in NOAH-MP LSM was recently evaluated over Southern Africa (Zhang et al., 2023). Our study complements the previous effort by evaluating the impact of combining the SoilGrids soil compositions with PTFs. Specifically, we focus on the impact of two different soil datasets on simulations of soil moisture and temperature during a period of normal and dry weather conditions.

2. Data and Methods

2.1 Background context of Ireland

https://doi.org/10.5194/hess-2023-304
Preprint. Discussion started: 30 April 2024
© Author(s) 2024. CC BY 4.0 License.

The Ireland is situated in a maritime temperate region where the climate is predominantly influenced by the mid-latitude westerly warm airflow off the North Atlantic Ocean, and occasional incursions of cold air masses during winter (Peel et al., 2007). The long-term (1981-2010) average daily maximum temperature of the region is between 18° and 20°C in summer and 8 °C in winter. Occasionally, the daily minimum temperature drops below 0 °C in winter. Rainfall is distributed throughout the year with mean annual value of 1200 mm. The west of Ireland typically experiences higher rainfall amounts (1000-1400 mm), and may exceed 2000 mm in the upland areas. Conversely, the east experiences lower rainfall amounts, between 750 and 1000 mm. More details on the background climate of Ireland are provided in Walsh (2012). In relation to the general soil information (Figure 1a), the south-east is characterized mainly by free draining sandy soils, peat soils dominate the mountains, hills and western edge of the country, while limestone-rich soils dominate the midlands and south (Creamer et al., 2014). Among the land cover types (Figure 1b), grassland dominates the agricultural and total land area in Ireland. The temperate climate in combination with fertile soils, mostly in the south and east where the soils are free draining, provides conditions that are favourable to near year round grass growth. However, the heavy clay (wet) soils limit grass growth in the west and north of the country (Keane and Collins, 2004).

2.2Model description

Here, we employ the advanced community NOAH-MP land surface model with multi-parameterization options, with improved representation of physical processes (Chen et al., 1996; Niu et al., 2011). The model is available as an uncoupled model, with the capacity to simulate different land state variables (e.g. soil moisture) and land energy, water and carbon fluxes. It also represents a LSM that is coupled with atmospheric models such as the Weather Research and Forecasting (WRF) model (Barlage et al., 2015). Due to its simplicity in selecting and combining multi-physics options, the model has been widely used for different applications, including natural hazards, drought and wildfire monitoring, land-atmosphere interactions, sensitivity and uncertainty quantification, biogeochemical processes, water dynamics, dynamic crop growth modeling, and soil hydrothermal processes. (Zhuo et al., 2019; Kumar et al., 2020; Chang et al., 2022; Hosseini et al., 2022; Nie et al., 2022; Warrach-Sagi et al., 2022; Hu et al., 2023).

In NOAH-MP LSM, the major improvements in mechanisms relevant to soil processes are (1) distinguishing less and more permeable frozen soil fractions, (2) introducing an

https://doi.org/10.5194/hess-2023-304
Preprint. Discussion started: 30 April 2024
© Author(s) 2024. CC BY 4.0 License.

alternative lower boundary soil temperature that is based on zero heat flux from the deep soil bottom, (3) adding TOPMODEL and SIMGM models for runoff and groundwater physics options (Niu et al., 2007), and (4) adding an unconfined aquifer beneath the 2 m bottom of the soil layer to account for water transport between the soil and aquifer. Relative to other LSMs, the NOAH-MP model framework is typical in its ability to define soil properties either by using dominant soil texture linked to empirically-derived soil parameter values, using soil texture with varying depths, or using soil texture compositions derived using PTFs (Saxton and Rawls, 2006).

The prognostic equations from Mahrt and Pan (1984) are used to describe soil moisture and soil temperature in the model (Chen et al., 1996).

$$C(\theta)\frac{\partial T}{\partial t} = \frac{\partial}{\partial z}\left(K_t(\theta)\frac{\partial T}{\partial z}\right) \quad (1),$$

$$\frac{\partial \theta}{\partial t} = \frac{\partial}{\partial z}\left(D\frac{\partial \theta}{\partial z}\right) + \frac{\partial K}{\partial z} + F_\theta \quad (2),$$

where C is the volumetric heat capacity, θ is the soil moisture, T is the soil temperature, and K and K_t are the hydraulic and thermal conductivities, respectively. D is the soil diffusivity and F_θ are the sinks and sources of soil water, that is, evaporation and precipitation.

2.3 Gridded data

Meteorological variables which are required as initial and forcing conditions are obtained from the European Centre for Medium-Range Weather Forecasting (ECMWF) database. We employ the state-of-the-art ECMWF ERA5-Land global reanalysis product that provides data at 0.1º (~9 km) spatial and hourly temporal resolution (Muñoz-Sabater, 2021). The required forcing variables include total precipitation, incident shortwave and longwave radiation, 2m air temperature, 10m zonal and meridional wind components, surface pressure and specific humidity. For initialisation, the model also requires input fields of soil temperature, surface skin temperature, canopy water and snow water equivalent at the first timestep. The hourly data for all variables was obtained for the period 2009-2022.

NOAH-MP model also requires static geographical data (e.g. soil texture and land use) and time varying vegetation products (e.g., leaf area index and fraction of green vegetation). We use the STATSGO gridded soil categories map provided at 5 arcmin resolution (~9 km) (FAO 2003a;b) and the International Soil Reference and Information Centre (ISRIC) global SoilGrids data (Hengl et al., 2017; Poggio et al., 2021). The latter is available at 250 m resolution and six standard soil depths, however, sand and clay proportions are currently available at four layers and provided as part of the WRF geographical data fields. Preprocessing of the data was undertaken in the WRF Preprocessing System (WPS) (Skamarock et al., 2019).

2.4 Model simulations

We set up and ran an offline NOAH-MP model version 4.3 within the framework of the High Resolution Land Data Assimilation System (HRLDAS) (Chen et al., 2007). Using the WPS system, the model domain is set up as a 1 km grid space covering the island of Ireland and the west coast of the United Kingdom (Figure 1). We incorporate a high resolution land use dataset based on the 100 m raster CORINE Land Cover for 2018 (CLC 2018). The 44 CORINE land cover classes are initially reclassified into 21 categories to match the default modified IGBP MODIS 20-category land use (Figure 1 b). The data is then resampled to 250 m. To generate the required geographic files for input to NOAH-MP, the CLC 2018 is converted to binary format which is used as input to the WPS, which subsequently generates the gridded geographic information required to run the NOAH-MP model. Other geographical data, such as topography, green vegetation fraction and surface albedo used in this study are derived from the model default datasets provided by the Research Application Laboratory, National Center for Atmospheric Research (RAL/NCAR).

To investigate the effect of soil hydrophysical properties on model simulations of soil moisture and soil temperature, we configure two experiments that are based on different soil data options, namely, (1) dominant soil texture categories used as default in WRF/NOAH-MP; and, (2) soil textural compositions in combination with PTFs (Saxton and Rawls, 2006). The dominant soil texture option uses the baseline FAO/STATSGO dataset with the empirically-derived soil properties from a look-up table, while the PTFs-derived soil properties use the fine-scale SoilGrids sand and clay proportions. The dominant topsoils across the domain are broadly classified into four and two broad categories based on STATSGO and SoilGrids, respectively (Figure 2). While Loam and Sandy Loam soil textures cover the largest area in both data sources (Table 2), the extent to which the difference in the data and soil physics options contribute to model uncertainty in NOAH-MP model is evaluated. Other NOAH-MP physics options used are outlined in Table 3.

For the numerical experiments, the soil layer thicknesses of 0.07, 0.21, 0.72 and 1.55 m are used, with a cumulative soil depth of 2.55 m. The thicknesses are selected to match the layers of initial soil input fields from ERA5-Land. The model is spun-up over 10 years for each experiment using the climatology of the hourly ERA5-Land for the period 2009-2022, to bring the soils to thermal and hydrologic equilibrium with the atmosphere. After spin-up, the model is assumed to be stable and is then used as the

https://doi.org/10.5194/hess-2023-304
Preprint. Discussion started: 30 April 2024
© Author(s) 2024. CC BY 4.0 License.
Hydrology and Earth System Sciences Discussions

point to initialise the simulations, reported on here, using the hourly meteorological forcing from 2009 to 2022.

2.5 Station data

Profile measurements of soil temperature and volumetric water content are obtained from two established eddy covariance grass flux sites, namely, Johnstown Castle and Dripsey (Kiely et al., 2018; Murphy et al., 2022), and five new sites (as part of the Terrain-AI project) at Athenry, Ballyhaise, Claremorris, Dunsany and Valentia. Terrain-AI is an on-going large-scale project, which in part focuses on establishing a long-term network of soil moisture monitoring sites across Ireland. It monitors and measures in situ soil moisture contents using Time Domain Reflectometry (TDR) sensors installed at different soil depths. Given that the Terrain-AI sites are new, the VWC measurements are so far limited to a year, and are prone to outliers because the TDR probes may require some time for the soil to settle and provide reliable measurements. In addition, the soil temperature measurements obtained from Met Eireann for the Terrain-AI sites are not homogenised or quality controlled. Despite the limitations of the observed data from the Terrain-AI sites, they are the only station observations available to evaluate our model results.

All the selected sites are distinguished by soil texture (Table 1) and contrasting soil water regimes (Figure 1 a). For example, Johnstown Castle site is characterized by seasonally dry and free draining sandy loam soils, whereas Dripsey is dominated by heavy soils that retains water throughout the year (e.g. Ishola et al., 2020). Half-hourly or hourly measurements are obtained for 2009-2012 period from Dripsey, 2018 (only second half of the year), 2019 and 2021 from Johnstown Castle, and the year 2022 for the Terrain-AI sites. Metadata for each station, outlining soil type, land cover and altitude are provided in Table 1.

2.6 Satellite products

Global satellite soil moisture datasets (e.g. ESA-CCI, SMAP, SMOS, and ASCAT) are often used to evaluate LSM at large spatial scales. Many of these products differ in terms of the satellite sensors and start of operations, and are subject to data gaps, coarse resolution and limited coverage (Beck et al., 2021). We use the Soil Water Index (SWI) products (soil moisture expressed in percentage degree of saturation) from the fusion of Sentinel-1 C-SAR and Metop ASCAT sensors to evaluate NOAH-MP model at grid scales. The product is produced from ASCAT surface soil moisture (SSM) using a two-layer water balance model that relates the surface and profile soil moisture as a function of time (Wagner, 1999; Albergel et al., 2008). We employ the

https://doi.org/10.5194/hess-2023-304
Preprint. Discussion started: 30 April 2024
© Author(s) 2024. CC BY 4.0 License.

operational ASCAT SWI provided at eight different time characteristics (taken as the soil depths), 1km resolution and daily mean values, from 2015 to 2022. The product is archived by Copernicus Land Service and has been well validated in previous studies (e.g. Albergel et al., 2012; Paulik et al., 2014; Beck et al., 2021).

2.7 Analysis

2.7.1 Model evaluation using in situ data

The half-hourly or hourly station data and model outputs for each grid cell are aggregated to daily averages to be consistent throughout the analysis. Then, for each validation site and variable, the daily mean values from the respective model grid cell are extracted at the model resolution. The daily values of soil temperature and volumetric water content (both at topsoil 0-7cm) layer are compared against the in situ measurements. The model estimated values are then evaluated using the Root Mean Square Deviation (RMSD), Percent Bias (PBIAS) and Pearson's Correlation Coefficient (R).

2.7.2 Model evaluation using satellite data

Given the limited number of in situ sites and scale differences between point observations and model grid resolution, the general interpretation of model performance across landscapes should be treated with care. However, the use of satellite data is a standard practice and a pragmatic way of evaluating model outputs of soil moisture over large spatial scales (He et al., 2023), notwithstanding the inherent uncertainty (e.g. coarse resolution and data gaps) of the satellite products. We evaluate NOAH-MP soil moisture output against ASCAT SWI for the surface and subsurface layers. To make the NOAH-MP soil moisture comparable with ASCAT SWI, we derive the grid-scale Relative Soil Moisture (RSM) to vary between 0 for wilting point and 1 for saturation (e.g. Samaniego et al., 2018)

$$RSM_{i,j,k} = \left(\frac{\theta_{i,j,k} - \theta_{wilt_{i,j}}}{\theta_{sat_{i,j}} - \theta_{wilt_{i,j}}}\right) x100 \qquad 3,$$

Where $\theta_{i,j,k}$ is the simulated volumetric water content, θ_{sat} and θ_{wilt} are the soil moisture at saturation and wilting point, respectively (Figure 3). We obtain RSM values for both the surface and subsurface soil layers. For the surface, ASCAT SWI-002 data, which imply the surface soil moisture conditions, are contrasted against the derived RSM values for the topmost soil depths of 3.5 cm. The subsurface RSM values are taken as the mean aggregates of the first three model layers, and are evaluated against ASCAT SWI-100. Similar metrics used for point-scale evaluation (see Section

© Author(s) 2024. CC BY 4.0 License.

2.7.1) are also calculated at grid scale between the reference datasets and model outputs for selected dry (2018) and normal (2019) years.

2.7.3 Soil moisture drought analysis

We also analyse the potential of NOAH-MP for monitoring the evolution of soil moisture drought across the domain. Since the west-central European summer drought of 2018 was an exceptional event in terms of hydrological extremes across Ireland (Met Éireann Report, 2018; Falzoi et al., 2019; Moore, 2020; Ishola et al., 2022), we evaluated the model over this period. We apply grid-scale cumulative RSM values integrated over three topmost soil layers (0-100 cm) (Section 2.7.2), due to its simplicity and ease in quantifying and interpreting available soil water. In principle, RSM is an important drought indicator, particularly at short-time scales, and analogous to the widely used Soil Moisture Index (SMI) for drought monitoring at different spatial scales (Samaniego et al., 2018; Grillakis, 2019).

To characterise soil moisture drought, percentiles of RSM values per grid cell are calculated based on 7-day windows from June to August for the climatology period 2009 - 2022. This amounts to 98 samples (7 days x 14 years) as input per window. For individual model experiments, STATSGO and SOILGRIDS, the derived spatial RSM percentiles per day in each window are then classified into different drought categories (Table 5), following Xia et al. (2014). These categories are currently being used by U.S. Drought Monitor (USDM) for operational and regionally specific drought monitoring (Svoboda et al., 2002).

3. Results

First, we present the analysis of ERA5-Land total annual precipitation in comparison with station data, to illustrate the level of uncertainty in input meteorology. Figure 4 shows that the seasonal variations and total annual cumulative of precipitation are reasonably replicated across the selected stations, and for different weather conditions, including the extended period of no rainfall in 2018 summer (Figure 4 f).

3.1Model evaluation: Soil moisture

Using station observations

The results of model simulations of volumetric water content (VWC in m^3 m^{-3}) for both STATSGO and SOILGRIDS are presented. Figures 5 and A1 illustrate the temporal comparisons and error statistics of VWC, respectively. It is important to note that we are comparing a model areal grid to a measurement point, which are assumed to be equivalent. The simulations are in closer agreement with the observed VWC at Athenry, Claremorris and Johnstown Castle with the lowest error statistics (RMSD ≈ 0.1 m^3 m^-

https://doi.org/10.5194/hess-2023-304
Preprint. Discussion started: 30 April 2024
© Author(s) 2024. CC BY 4.0 License.

^{3}, PBIAS < 25%) relative to other stations (Figure A1). The lowest model performance occurs at Dunsany, Valentia and Dripsey, with RMSD > 0.15 m^3 m^{-3}, PBIAS > 30%. The Pearson's correlation is generally high, above 0.8, across the measurement sites except for Ballyhaise and Claremorris. Both experiments broadly underestimate the observed VWC values, but the model bias is lower in the STATSGO than the SOILGRIDS experiment, consistent across the stations (Figure A1). These dry biases (0.15 - 0.4 m^3 m^{-3}) are broadly dominated in autumn and winter during which the VWC values are higher or soil is assumed to be relatively wetter (Figure 5 a-f), except at Dripsey where the dry biases are systematic throughout the years (Figure 5g). Conversely, in summer where soil moisture conditions tend to dry in response to atmospheric changes (e.g. higher global solar radiation and evaporation), VWC temporal patterns are adequately captured by both model experiments (biases are less than 0.1 m^3 m^{-3}), including the 2018 exceptionally dry summer soil moisture content (Figure 5f). The differences between STATSGO and SOILGRIDS are relatively small (< 0.05 m^3 m^{-3}) across the year(s).

Figure 5 (boxplot) further illustrates the summary statistics and spread of model simulations and observed VWC. The mean of observed VWC (≈0.3 m^3 m^{-3}) is better captured in STATSGO than the SOILGRIDS, particularly at Athenry, Ballyhaise, Claremorris and Johnstown Castle. However, with the mean of observed VWC exceeding this value, both experiments lead to significant underestimation of VWC, as evident at Dunsany, Valentia and Dripsey.

Overall, the model experiments closely replicate both the mean and variance of the measured surface VWC values at Athenry, Claremorris and Johnstown Castle locations, where the soils are either well- or imperfectly-drained (Figure 1a).

Using reference ASCAT satellite SWI data

The selected measurement stations are well distributed and represent different soil moisture regimes across Ireland (Figure 1a). However, given the relatively small number of stations, generalizing the results to the entire domain may be erroneous. Instead, model grid cells are individually evaluated against the reference ASCAT satellite data. Figure 6 shows the results of all Ireland grid-scale model evaluation of daily derived RSM values against the reference SWI at the surface and subsurface for 2018 dry and 2019 normal years. Median metrics for each soil texture category in STATSGO and SOILGRIDS are presented in Tables 5 and 6.

As shown in Figure 6 (top) for the 2018 dry year, model performance is broadly better for STATSGO than for SOILGRIDS, with lower median (black crossbar); RMSD of around 0.015%, PBIAS of 1% in magnitude of ASCAT SWI, for both surface and

https://doi.org/10.5194/hess-2023-304
Preprint. Discussion started: 30 April 2024
© Author(s) 2024. CC BY 4.0 License.

subsurface RSM grid values. While the Pearson's R statistic (median around 0.85) for STATSGO and SOILGRIDS is comparable for the surface layer, the SOILGRIDS experiment produces a higher R value in the subsurface layer during the dry year. For the 2019 normal year (Figure 6, bottom), the spatial distribution of error statistics at the surface layer is nearly similar for both experiments, with median RMSD of 0.015 %, PBIAS of around 6 % (1 % for SOILGRIDS) and R of 0.73. At the subsurface layer, SOILGRIDS produces better results than STATSGO with lower RMSD (0.01 %) and PBIAS (6%) distributions and higher R statistics (median around 0.76).

The extended tails (positive/negative in PBIAS and lower/higher in RMSD and R) in the density distribution indicate a relatively small number of isolated (spatial) grid cells with larger error statistics. Given that the Loam (L) and Sandy Loam (SL) soils represent the largest proportion of grid cells across the study domain and are relatively comparable in terms of spatial coverage in STATSGO and SOILGRIDS (Table 2), the error statistics for these soil texture categories are explained here. For 2018, results show that both experiments produce lower RMSD and PBIAS error statistics for SL than L at the surface layer (Table 5). Whereas at the subsurface layer, SOILGRIDS perform better than STATSGO for both soil categories. For the 2019 normal year (Table 6), STATSGO gives lower RMSD and PBIAS error statistics than SOILGRIDS at the surface layer. Overall, model performs better over L soil type than SL based on the lower PBIAS and higher R values. The RMSD and R statistics are relatively comparable at the subsurface layer for both the STATSGO and SOILGRIDS simulations and for L and SL soil categories. However, STATSGO produces lower PBIAS statistics than SOILGRIDS in L soil. Generally, the error statistics are lower in L than SL soil at the sub surface layer.

The spatial characteristics of model surface RSM annual mean bias relative to the reference datasets for the years 2018 and 2019 are illustrated in Figure 7 a-j, and the long-term seasonal characteristics of topsoil VWC between the experiments are shown in Figure A2. Wet biases are predominant in the north, characterised as SL in STATSGO and SOILGRIDS; towards the south and southeast of the domain, the results shift towards a dry bias, mostly in areas represented by L soils. While the spatial coverage of model bias is consistent for both experiments and the years, the dry bias in both years is more pronounced in SOILGRIDS than STATSGO in the affected areas. Conversely, the wet bias is more widespread in STATSGO than SOILGRIDS.

3.2Model evaluation: Soil temperature

Figure 8 (a-g) illustrates model comparisons against the reference station measurements of top soil temperature, while Figure A3 shows the associated

https://doi.org/10.5194/hess-2023-304
Preprint. Discussion started: 30 April 2024
© Author(s) 2024. CC BY 4.0 License.

evaluation results. Generally, the error statistics (RMSD and PBIAS) for both the STATSGO and SOILGRIDS experiments are low, and R values are high (above 0.9 across all sites). The model errors are better RMSD < 3 K and PBIAS < 1% in Athenry, Dunsany, Valentia and Johnstown Castle, than in Ballyhaise, Claremorris and Dripsey where the errors exceeded these values. Comparatively, SOILGRIDS leads to a slightly better model performance than STATSGO across the sites.

Additionally, the soil temperature increases from around 280 K in winter to a peak of about 297 K in summer , and up to 300 K during the extreme hot and dry summer of 2018 (e.g. Johnstown Castle) (Figure 8f). The spread and variance of the observed soil temperature are reasonably replicated by both experiments (Figure 8, bottom). Whereas the mean of observed soil temperature, which is approximately 285 K, is systematically underestimated by 1 K to 3 K across stations, the peak values in the mid-summer months are well captured by the experiments (Figure 8a-g).

Overall, both STATSGO and SOILGRIDS produce soil temperature profiles that are close, but significantly different (*p-value* $< 2.2 \times 10^{-16}$) and are comparable with observations for the study year(s) and locations.

Given the reasonable model performance across the selected locations, the grid-scale model differences between STATSGO and SOILGRIDS in the absence of satellite reference observations, is further examined (Figure 9). The spatial differences of surface soil temperature are based on the seasonal long-term climatology from 2009 to 2022. In response to seasonal variations in global solar radiation and VWC, winter shows the lowest soil temperature (Figure 9 a,e,i), whereas summer is characterised by the highest soil temperature (Figure 9 c,g,k). The highest soil temperature in summer are widespread mostly over Loam soil in the south and southeast of the study domain. The south and east are seasonally drier, experiencing lower rainfall and soil water deficits in summer (Figures 1a and A4). In other seasons, the spatial characteristics are irregular. This spatiotemporal evolution of the soil temperature characteristics is consistent in both STATSGO and SOILGRIDS model experiments. That is, both soil texture maps produce soil temperature differences that are negligible mostly in the south and southeast dominated by Loam soils (Figure 9 i-l). However, STATSGO broadly shows a cold soil temperature bias in Clay and Clay Loam soils, and a small warm bias over Sandy Loam in the northern border and southwest, relative to SOILGRIDS. The areas of cold and warm biases broadly coincide with areas of wet and dry biases of STATSGO VWC in comparison with SOILGRIDS (Figure A2).

3.3 Spatial and temporal evolution of soil moisture drought

https://doi.org/10.5194/hess-2023-304
Preprint. Discussion started: 30 April 2024
© Author(s) 2024. CC BY 4.0 License.

Figure 10 illustrates the spatial characteristics of 0-100 cm RSM percentiles for selected days during summer 2018. The days are used to denote the start, peak and end of summer water deficits (Figure 4 f). For the first 7-day window ending 07 June, the southeast and east of Ireland broadly show low drought intensity D0-D1 (abnormal/moderate) in STATSGO, relative to SOILGRIDS with severe drought D2 category. Both experiments are largely consistent in other areas of the study domain. For example, the major land areas in the north of the island are characterised as severe drought D2, and D0-D1 in the midlands and west of Ireland. However, the D0-D1 categories are more spatially widespread across the midlands and west in SOILGRIDS than in STATSGO.

By the middle of summer 2018 (sixth week ending 12 July), the entire Ireland is dominated by exceptional drought D4 category in STATSGO, except for the land areas in the north where the D2 category is sustained over time. These patterns are consistent in SOILGRIDS except for some areas with higher intensity. For example, the drought category in the southeast of Northern Ireland shifts from D2 in STATSGO to D3-D4 (extreme and exceptional) categories, and from D2-D3 (severe and extreme) category in the southwest of Ireland to D3-D4 drought categories in SOILGRIDS.

Whereas the soil water deficits appear to have improved by the end of summer (week 13 ending 30 August), the landscapes are still largely under different levels of soil dryness. For example, in STATSGO, moderate drought D1 category broadly dominates the Loam soil texture areas in the midlands, south and southeast of Ireland, while a mix of drought D1-D4 categories dominates the west and southwest of the country. These patterns are consistent in SOILGRIDS, but areas in the northern border, west and southwest with a sustained D3-D4 categories are wider in SOILGRIDS than STATSGO.

Figure 11 illustrates the time-areal coverage cross-section of various drought categories over the domain during the summer period 2018, based on RSM percentiles. While the landscapes are already under soil water deficits by the start of summer in June, the largest areal coverage (about 70 % in STATSGO and 80 % in SOILGRIDS) is dominated by low drought intensities (D0-D2). Approximately 10 % of the domain is characterised by extreme and exceptional D3-D4 drought, up to the end of June. The drought intensifies effectively from late June, with higher areal coverage of D4 category of more than 80 %, extending for several days in STATSGO. This is similar in SOILGRIDS, however, days in July that show recovery based on a reduced areal coverage of D3-D4 category in STATSGO, show high coverage of the same intensities in SOILGRIDS. At the start of August, the areal coverage of high intensity D3-D4 drought has effectively dropped, compensated by an increase in the spatial coverage of D0-D2. In the last week of August, the areal coverage of D0-D1 is higher (about 80 %) relative to other drought categories.

4. Discussions

4.1 Effects of soil hydrophysical properties on simulated soil hydrothermal regimes.

As a consequence of misrepresentation of soil texture classes in LSMs, soil hydrophysical properties are expected to influence model simulations of changes in soil moisture content and soil temperature across space and time. In this study, we investigate the difference between two commonly used global soil texture maps implemented in NOAH-MP land surface model, namely STATSGO and SOILGRIDS. The impact of using the default look-up table and PedoTransfer Functions (PTFs) to prescribe grid-scale soil properties (e.g. porosity, field capacity, wilting point, hydraulic conductivity, etc.), on simulated surface and subsurface soil hydrothermal changes during normal period and extremely dry year is further evaluated. The role of these properties, particularly the field capacity – a measure of water retained in the soil at the pressure of -0.33 bar, after excess rain water has drained off, are critical in LSMs that simulate soil hydrophysical processes and interactions with the atmosphere.

At point-scale, the results reveal model differences between dry and wet soil moisture regimes and are able to fairly replicate the measured values of soil moisture and soil temperature across a variety of weather conditions, including during extreme water shortage. While STATSGO is closer to observations than SOILGRIDS, the model errors between these data sources are marginal but statistically significant (*p-value* $< 2.2 \times 10^{-16}$) for both variables, notwithstanding the difference in soil physics. Despite misrepresentation of soil texture class by both sources, for example at Johnstown Castle (Table 1), the model does reasonably well. However, for a relatively wet site (e.g. Dripsey) where the soil texture class is accurately represented in both soil databases, the model systematically underestimates soil moisture content (Figures 5g and A1). This illustrates that the soil-induced model uncertainty is rarely linked to misrepresentation of soil texture class, but to the soil physics and the prescribed soil hydrophysical parameters.

For example, the field capacity (FC) value reported for Johnstown Castle (Table 1) is 0.32 $m^3 m^{-3}$ (Ishola et al., 2020), which is close to the values employed in STATSGO and SOILGRIDS, and consistent with station measurements (Figures 3 and 4). However, the observed FC value in Dripsey is approximately 0.42 $m^3 m^{-3}$ (Table 1), which contrasts the values of approximately 0.31 $m^3 m^{-3}$ used in the models (Figure 3 and 4 bottom) and values reported in Liu et al. (2012) and Ishola et al. (2020) for this site. The bias in FC limits the ability of the soil to increase the memory of the stores,

https://doi.org/10.5194/hess-2023-304
Preprint. Discussion started: 30 April 2024
© Author(s) 2024. CC BY 4.0 License.

Hydrology and Earth System Sciences
Discussions

resulting in systematic bias in the simulated VWC. To illustrate the role of prescribed FC values for Dripsey, the simulated VWC for a neighboring grid cell with a FC of 0.412 m^3 m^{-3} and similar weather condition is evaluated against the measured VWC (Figure 12). A higher FC clearly results in higher VWC values, reducing the bias between observations and STATSGO by more than 50 % of the value at Dripsey. In contrast, the maximum FC derived from SOILGRIDS across the domain is 0.34 m^3 m^{-3} (Figure 3), which still lies around the default value, and is not in a proximal grid location to Dripsey site. Hence, using the same grid cell as above, the SOILGRIDS with PTFs fall short of this illustration and consequently fail to improve the simulated VWC.
At grid-scale, the STATSGO and SOILGRIDS soil texture data are evidently different, particularly in the north, west and southwest of Ireland (Figure 2). Notably, the STATSGO data represents smaller soil grain sizes in most of these areas, relative to SOILGRIDS. This results in higher values of soil hydrophysical properties in STATSGO, including porosity and field capacity (Figure 3). The increasing grain size leads to wet and cold biases in STATSGO, relative to SOILGRIDS in these notable areas (Figures 7, 9 and A2). Similar to our results, It has been demonstrated that a reduction in soil grain size (e.g. Loam to Sandy Loam) leads to dry and hot biases (decrease in latent heat flux and increase in sensible heat flux) between two global soil datasets (Dennis and Berbery, 2021).

While the choice of PTFs is critical in model simulations of soil water fluxes (Weihermüller et al. 2021), the default Saxton and Rawls (2006) soil physics produce properties that are very close to using the look-up table in NOAH-MP model. One reason for this similarity is that the SOILGRIDS sand and clay compositions produce Loam and Sandy Loam soil texture, based on USDA classes, and these coincide with FAO/STATSGO in space with nearly the same areal coverage (Figure 2 and Table 2). Another reason for similar soil properties between the PTFs and look-up table, is the default PTFs coefficients which are derived based on USDA soil samples (Saxton and Rawls, 2006) and may be inaccurate for the study domain; the empirically-derived look-up table is also based on soil samples in the US. The net effect of similar but inaccurate soil properties is the significant under-representation of soil hydrothermal regimes in wet soils as illustrated in Figures 5 and 7. This aligns with Vereecken et al. (2010) who demonstrated that PTFs are highly accurate over the areas for which they have been developed, but have limited accuracy if transferred outside these areas.
The overall results indicate that there is a major impact of under-represented soil hydrophysical parameters, particularly in relatively wet sites, regardless of the source of global soil texture map and soil physics option implemented in NOAH-MP. The

discrepancies between STATSGO and SOILGRIDS exert great regional impacts on the soil hydrothermal regimes.

4.2 Implications for regional drought monitoring

Soil moisture content is an essential variable in many hydrological applications and in understanding the evolution and characteristics of extreme climate events such as droughts. Instead of heatwaves, the study domain is rather subject to rainfall extremes (Noone et al., 2017), a precursor of soil water deficits and droughts; the intensity and frequency of which have been projected to increase globally and in the study domain by the end of century (Seneviratne et al., 2012; Fealy et al., 2018).

In this study, the drought analysis are based on the cumulative RSM percentiles aggregated over three uppermost soil layers (0-100 cm) for 2018 summer hydrological extremes for STATSGO and SOILGRIDS (Figures 10-11). The 0-100 cm depth is sufficient for drought assessment since the root zone of many crops grown across the world does not surpass 1.0 m in depth (Fan et al., 2016; Grillakis et al., 2019).

Both STATSGO and SOILGRIDS are largely consistent in terms of the evolution of soil moisture drought in space and time. However, SOILGRIDS shows higher drought intensity in the many areas, relative to STATSGO. This is due to the dry bias of SOILGRIDS associated with underrepresented soil hydrophysical properties and simulated VWC (Figures 3 and A2). During the summer of 2018, particularly from late May to late July, Ireland was reported to have experienced different degrees of meteorological droughts (rainfall deficits) (Figure 4 f) ranging from dry spells to absolute droughts (Met Éireann Report, 2018; Falzoi et al., 2019; Moore, 2020). Meteorological droughts precede soil moisture/agricultural droughts through reduction in soil water storage and available water for plant uptake, our results indicate that extreme to exceptional soil moisture droughts are only effective from last week in June, covering the large part of the domain by mid-July (Figure 11). During August, rainfall improved soil water stores (Figure 4 f) and weakened drought conditions across much of the country, particularly in the north and west (Met Éireann Report, 2018; Moore, 2020).

Overall, the discrepancies between STATSGO and SOILGRIDS impacts drought characteristics mostly in space, with SOILGRIDS shifting the abnormal/moderate/severe droughts in STATSGO to extreme/exceptional droughts. These may result in erroneous or potential loss of vital information with dire consequences on ecosystems with regards to predicting the response and productivity, as drought stress has been highlighted as the primary factor limiting ecosystem response and productivity (De Boeck et al., 2011).

https://doi.org/10.5194/hess-2023-304
Preprint. Discussion started: 30 April 2024
© Author(s) 2024. CC BY 4.0 License.

5. Conclusions

In this study, the usability of two global soil datasets for representing soil processes in NOAH-MP model and simulating soil hydrothermal variations and associated extremes, has been evaluated across all of Ireland. Specifically, FAO/STATSGO dominant soil texture categories linked to an empirically-derived soil hydrophysical properties from a look-up table (default in WRF), are compared with PedoTransfer Functions (PTFs) that ingest an alternative SOILGRIDS sand and clay compositions at four soil layers. Through temporal comparison with in situ soil moisture and soil temperature observations, it has been found that, both soil datasets can fairly replicate the general soil hydrothermal variations. However, they under-represent the soil properties (e.g. field capacity) in wet loam soil, leading to systematic dry bias in soil moisture. The results have further shown that there is no distinct difference between the soil physics applied to the same soil texture category in both STATSGO and SOILGRIDS. But, the disparities and sensitivity to soil physics increase for different soil texture categories between the datasets.

Through spatial comparison with satellite-based ASCAT SWI, dry bias is more pronounced and widespread in the midland, south and east in SOILGRIDS, while wet bias dominates the west and north. As a consequence, 2018 summer soil moisture droughts broadly intensify more in SOILGRIDS than in STATSGO. These disparities may result in misinformation that could hamper adequate and effective preparation and response during drought episodes. While identifying the better soil database is not the primary objective of this study, STATSGO performs slightly better than SOILGRIDS. Overall, the study highlights the shortcomings of global soil databases in simulating soil hydrothermal changes and underscore the need to optimize and improve global soil hydrophysical properties that are ingested in LSMs for better performance. Developing detailed regional soil texture properties may be more realistic and enables more improvement in model simulations. Ultimately, this would advance the understanding of the role of soil processes in hydrologic cycle, ecosystem productivity, drought evolution, land-atmosphere interactions and regional climate.

A number of initiatives (e.g. Terrain-AI) has been developed to deploy soil moisture measuring network across Ireland to address the lack of soil moisture observations. A significant conclusion of this study is that the NOAH-MP model has shown an excellent capacity to ingest better alternative soil texture data, to reduce the model biases of soil hydrothermal changes and evolution of soil moisture drought. Therefore, it can be applied to augment current network of sites across the country for operational modeling

© Author(s) 2024. CC BY 4.0 License.

and real-time forecasting of soil moisture conditions and drought across the domain. This will support hydrometeorological monitoring similar to Global Food Awareness System (GloFAS) and NASA's Short-term Prediction Research and Transition with Land Information System (SPoRT-LIS).

Code and data availability

The open-source HRLDAS/NOAH-MP model is freely available on github (https://github.com/NCAR/hrldas). The ERA5-Land hourly input meteorological forcing were downloaded from the climate data store (https://cds.climate.copernicus.eu/). The WPS geographical data were downloaded from NCAR (https://ral.ucar.edu/model/noah-multiparameterization-land-surface-model-noah-mp-lsm). 2018 Corine land use and satellite ASCAT soil water index are freely available on Copernicus Global Land Service (https://land.copernicus.eu/global/index.html). In situ data for the selected sites were obtained from Met Eireann, Ireland and from the European fluxes database cluster (http://www.europe-fluxdata.eu).

Competing interests

The contact author has declared that none of the authors has any competing interests.

Acknowledgments

We thank Gary Lanigan for granting access to measurements from Johnstown Castle. Computing resources for model runs in this work were provided by the Microsoft Azure high performance computers. This research under the Terrain-AI project (SFI 20/SPP/3705) has been supported by Science Foundation Ireland Strategic Partnership Programme and co funded by Microsoft.

Author Contributions

Conceptualization, K. I. and R. F.; methodology, K.I. and R.F.; software, K.I. and R. F, with contributions by P. L. and D. W. ; validation, K. I..; formal analysis, K. I.; investigation, K. I.; resources, K.I. and R.F.; data curation, K. I.; writing—draft preparation and review, was led by K. I., G. M., M.D. and R. F., with contributions from all co-authors.; visualization, K.I.; supervision, R.F. and G. M.; project administration, R.F. and T.M.; funding acquisition, R.F. and T.M.

References

Albergel, C., Rüdiger, C., Pellarin, T., Calvet, J.-C., Fritz, N., Froissard, F., Suquia, D., Petitpa, A., Piguet, B., and Martin, E.: From near-surface to root-zone soil moisture using an exponential filter: an assessment of the method based on in-situ observations and model simulations, *Hydrol. Earth Syst. Sci.*, 12, 1323–1337, https://doi.org/10.5194/hess-12-1323-2008, 2008

Albergel, C., de Rosnay, P., Gruhier, C., Muñoz-Sabatera, J., Hasenauer, S., Isaksen, L., Kerr, Y., and Wagner, W.: Evaluation of remotely sensed and modelled soil moisture products using global ground-based in situ observations, *Remote Sens. Environ.*, 118, 215–226, https://doi.org/10.1016/j.rse.2011.11.017,2012

Arsenault, K. R., Nearing, G. S., Wang, S., Yatheendradas, S., and Peters-Lidard, C. D.: Parameter sensitivity of the Noah-MP land surface model with dynamic vegetation. *J. Hydrometeorol.* 19, 815–830. doi: 10.1175/jhm-d-17-0205.1,2018

Barlage, M., Tewari, M., Chen, F., Miguez-Macho, G., Yang, Z.-L., & Niu, G.-Y.: The effect of groundwater interaction in North American regional climate simulations with WRF/Noah-MP. *Climatic Change*, 129(3–4), 485–498. https://doi.org/10.1007/s10584-014-1308-8, 2015

Beck, H. E., Pan, M., Miralles, D. G., Reichle, R. H., Dorigo, W. A., Hahn, S., Sheffield, J., Karthikeyan, L., Balsamo, G., Parinussa, R. M., van Dijk A. I. J. M., Du, J., Kimball, J. S., Vergopolan, N., Wood, E. F.: Evaluation of 18 satellite- and model-based soil moisture products using in situ measurements from 826 sensors. *Hydrology and Earth System Sciences*, **25**(1), 17– 40. https://doi.org/10.5194/hess-25-17-2021, 2021

Blyth, E.M., Arora, V.K., Clark, D.B., Dadson, S. J., De Kauwe, M. G., Lawrence, D. M., Melton, J. R., Pongratz, J., Turton, R. H., Yoshimura, K., Yuan, H.: Advances in Land Surface Modelling. *Curr Clim Change Rep* **7**, 45–71. https://doi.org/10.1007/s40641-021-00171-5, 2021

Chang, M., Cao, J., Zhang, Q., Chen, W., Wu, G., Wu, L., Wang, W., Wang, X.: Improvement of stomatal resistance and photosynthesis mechanism of Noah-MP-WDDM (v1.42) in simulation of NO2 dry deposition velocity in forests, *Geoscientific. Model Development*, 15, 787-801, https://doi.org/10.5194/gmd-15-787-2022, 2022

Chen, F., Mitchell, K., Schaake, J., Xue, Y., Pan, H. L., Koren, V., Duan, Q. Y., Ek, M., Betts, A.: Modeling of land surface evaporation by four schemes and comparison with FIFE observations. *Journal of Geophysical Research*, **101**, 7251– 7268. https://doi.org/10.1029/95JD02165, 1996

Chen, F., Manning, K. W., Lemone, M. A., Trier, S. B., Alfieri, J. G., Roberts, R., Tewari, M., Niyogi, D., Horst, T. W., Oncley, S. P., Basara, J. B., and Blanken, P. D.: Description and evaluation of the characteristics of the NCAR high-resolution land data assimilation system, *J. Appl. Meteorol. Clim.,* 46, 694–713, https://doi.org/10.1175/JAM2463.1, 2007

Creamer, R.E., Simo, I., Reidy, Carvalho, J., Fealy, R., Hallett, S., Jones, R., Holden, A., Holden, N., Hannam, J., Massey, P., Mayr, T., McDonald, E., O'Rourke, S., Sills, P., Truckell, I., Zawadzka, J. and Schulte, R.P.O. 2014. Irish Soil Information System. Synthesis Report (2007-S-CD-1-S1). EPA STRIVE Programme, Wexford.

Dai, Y., Shangguan, W., Wei, N., Xin, Q., Yuan, H., Zhang, S., Liu, S., Lu, X., Wang, D., Yan, F:. A review of the global soil property maps for Earth system models, *Soil*, 5, 137-158, https://doi.org/10.5194/soil-5-137-2019, 2019a

Dai, Y., Xin, Q., Wei, N., Zhang, Y., Shangguan, W., Yuan, H., Zhang, S., Liu, S., Lu, X.: A global high-resolution data set of soil hydraulic and thermal properties for land surface modeling, *J. Adv. Model. Earth Syst*., 11, 2996-3023, https://doi.org/10.1029/2019MS001784, 2019b

De Boeck, H.J., Dreesen, F. E., Janssens, I. A., Nijs, I.: Whole-system responses of experimental plant communities to climate extremes imposed in different seasons. *New Phytologist*, 189, 806-817. doi: 10.1111/j.1469-8137.2010.03515.x, 2011

de Lannoy, G. J. M., R. D. Koster, R. H. Reichle, S. P. P. Mahanama, and Q. Liu: An updated treatment of soil texture and associated hydraulic properties in a global land modeling system. *J. Adv. Model. Earth Syst.*, 6, 957–979, https://doi.org/10.1002/2014MS000330, 2014

https://doi.org/10.5194/hess-2023-304
Preprint. Discussion started: 30 April 2024
© Author(s) 2024. CC BY 4.0 License.

Dennis, E. J., Berbery, E. H.: The role of soil texture in local land surface-atmosphere coupling and regional climate, *J. Hydromet.*, 22, 313-330, https://doi.org/10.1175/JHM-D-20-0047.1, 2021

Dennis, E. J., Berbery, E. H.: The effects of soil representation in WRF-CLM on the atmospheric moisture budget, *J. Hydromet.*, 23, 681-696, https://doi.org/10.1175/JHM-D-21-0101.1, 2022

Falzoi, S., Gleeson, E., Lambkin, K., Zimmermann, J., Marwaha, R., O'Hara, R., Green, S. and Fratianni, S.: Analysis of the severe drought in Ireland in 2018. *Weather*, 99, 1–6. https://doi.org/10.1002/wea.3587, 2019

Fan, J., B. McConkey, H. Wang, H. Janzen: Root distribution by depth for temperate agricultural crops, *Field Crop Res*., 189, 68-74, 10.1016/J.FCR.2016.02.013, 2016

FAO: Digital soil map of the world and derived soil properties, FAO, Land and Water Digital Media Series, CD-ROM., 2003a

FAO: The Digitized Soil Map of the World Including Derived Soil Properties (version 3.6), FAO, Rome, Italy, 2003b

Fealy, R. Bruyére, C., Duffy, C.: Regional Climate Model Simulations for Ireland for the 21st Century, Final Report. Environmental Protection Agency, Co. Wexford, 1-137, 2018

Fisher, R. A., Koven, C. D.: Perspectives on the Future of Land Surface Models and the Challenges of Representing Complex Terrestrial Systems, *J. Adv. Model. Earth Sys.*, 12, e2018MS001453, https://doi.org/10.1029/2018MS001453, 2020

Gee, G.W., Bauder, J.W.: Particle-size Analysis, in: Klute, A. (Ed.), SSSA Book Series. Soil Science Society of America, American Society of Agronomy, Madison, WI, USA, pp. 383–411. https://doi.org/10.2136/sssabookser5.1.2ed.c15, 2018

Grillakis, M. G.: Increase in severe and extreme soil moisture droughts for Europe under climate change, *Science of the Total Environment*, 660, 1245-1255, https://doi.org/10.1016/j.scitotenv.2019.01.001, 2019

He, J. J., Y. Yu, L. J. Yu, C. M. Yin, N. Liu, S. P. Zhao, and X. Chen: Effect of soil texture and hydraulic parameters on WRF simulations in summer in east China. *Atmos. Sci. Lett.*, **17**, 538–547, https://doi.org/10.1002/asl.690, 2016

He, Q., Lu, H., Yang, K.: Soil Moisture Memory of Land Surface Models Utilized in Major Reanalyses Differ Significantly from SMAP Observation, *Earth's Future*, 11, e2022EF003215, https://doi.org/10.1029/2022EF003215, 2023

Hengl, T., Mendes de Jesus, J., Heuvelink, G. B. M., Ruiperez Gonzalez, M., Kilibarda, M., Blagotic, A., Shangguan, W., Wright, M. N., Geng, X., Bauer-Marschallinger, B., Guevara, M. A., Vargas, R., MacMillan, R. A., Batjes, N. H., Leenaars, J. G. B., Ribeiro, E., Wheeler, I., Mantel, S., and Kempen, B.: SoilGrids250m: global gridded soil information based on Machine Learning, *PLOS One,* 12, e0169748, https://doi.org/10.1371/journal.pone.0169748, 2017

Hosseini, A., Mocko, D. M., Brunsell, N. A., Kumar, S. V., Mahanama, S., Arsenault, K., Roundy, J. K. : Understanding the impact of vegetation dynamics on the water cycle in the NOAH-MP model, *Front. Water*, 4, 2022, https://doi.org/10.3389/frwa.2022.925852 , 2022

Hu, W., Ma, W., Yang, Z.-L., Ma, Y., and Xie, Z.: Sensitivity analysis of the Noah-MP land surface model for soil hydrothermal simulations over the Tibetan Plateau. *Journal of Advances in Modeling Earth Systems*, 15, e2022MS003136. https://doi. org/10.1029/2022MS003136, 2023

© Author(s) 2024. CC BY 4.0 License.

Ishola, K.A., Mills, G., Fealy, R.M., Ní, C.Ó. and Fealy, R.: Improving a land surface scheme for estimating sensible and latent heat fluxes above grassland with contrasting soil moisture zones. *Agricultural and Forest Meteorology*, 294,108151. https://doi.org/10.1016/j.agrformet.2020.108151, 2020

Ishola, K. A., Mills, G., Fealy, R. M., Fealy, R.: A model framework to investigate the role of anomalous land surface processes in the amplification of summer drought across Ireland during 2018, *International Journal of Climatology*, 43, 480 - 498. https://doi.org/10.1002/joc.7785, 2022

Jordan, R.: A one-dimensional temperature model for a snow cover: Technical documentation for SNTHERM 89, US Army Cold Regions Research and Engineering Laboratory Special Report 91-16, 49, 1991

Keane, T. and Collins, J.F. (Eds.).: Climate, Weather and Irish Agriculture, AGMET, UCD, Belfield, Dublin 4, 2004

Kiely, G., Leahy, P., Lewis, C., Sottocornola, M., Laine, A., Koehler, A.-K.: GHG Fluxes from Terrestrial Ecosystems in Ireland. Research report No. 227.EPA Research Programme, Wexford. Available online at https://www.epa.ie/pubs/reports/research/climate/Research_Report_227.pdf, 2018

Kishné, A. S., Y. T. Yimam, C. L. S. Morgan, and B. C. Dornblaser: Evaluation and improvement of the default soil hydraulic parameters for the Noah land surface model. *Geoderma*, 285, 247–259, https://doi.org/10.1016/j.geoderma.2016.09.022, 2017

Kumar, S. V., Holmes, T. R., Bindlish, R., de Jeu, R., and Peters-Lidard, C.: Assimilation of vegetation optical depth retrievals from passive microwave radiometry, *Hydrol. Earth Syst. Sci.,* 24, 3431–3450, https://doi.org/10.5194/hess-24-3431-2020, 2020

Lehmann, P., O. Merlin, P. Gentine, and D. Or: Soil texture effects on surface resistance to bare-soil evaporation. *Geophys. Res. Lett.*, **45**, 10 398–10 405, https://doi.org/10.1029/2018GL078803, 2018

Li, J., Chen, F., Zhang, G., Barlage, M., Gan, Y., Xin, Y., Wang, C.: Impacts of land cover and soil texture uncertainty on land model simulations over the Central Tibetan Plateau, *J. Adv. Model. Earth Syst.*, 10, 2121-2146, https://doi.org/10.1029/2018MS001377, 2018

Liu, W., Xu, X. and Kiely, G.: Spatial variability of remotely sensed soil moisture in a temperate-humid grassland catchment. *Ecohydrol.*, 5: 668-676. https://doi.org/10.1002/eco.254, 2012

Looy, K. V., Bouma, J., Herbst, M., Koestel, J., Minasny, B., Mishra, U., Montzka, C., Nemes, A., Pachepsky, Y. A., Padarian, J., Schaap, M. G., Tóth, B., Verhoef, A., Vanderborght, J., Ploeg, M. J., Weihermüller, L., Zacharias, S., Zhang, Y., and Vereecken, H.: Pedotransfer Functions in Earth System Science: Challenges and Perspectives, *Rev. Geophys.*, 55, 1199–1256, https://doi.org/10.1002/2017RG000581, 2017

Luo, Y., Ahlström, A., Allison, S. D., Batjes, N. H., Brovkin, V., Carvalhais, N., Chappell, A., Ciais, P., Davidson, E. A., Finzi, A., Georgiou, K., Guenet, B., Hararuk, O., Harden, J. W., He, Y., Hopkins, F., Jiang, L., Koven, C., Jackson, R. B., Jones, C. D., Lara, M. J., Liang, J., McGuire, A. D., Parton, W., Peng, C., Randerson, J. T., Salazar, A., Sierra, C. A., Smith, M. J., Tian, H., Todd-Brown, K. E. O., Torn, M., van Groenigen, K. J., Wang, Y. P., West, T. O., Wei, Y., Wieder, W. R., Xia, J., Xu, X., Xu, X., and Zhou, T. C. G. B.: Toward more realistic projections of soil carbon dynamics by Earth system models, *Global Biogeochem. Cy*., 30, 40–56, https://doi.org/10.1002/2015gb005239, 2016

Mahrt, L., and K. Ek: The influence of atmospheric stability on potential evaporation. *J. Climate Appl. Meteor.*, **23 ,** 222–234, 1984

https://doi.org/10.5194/hess-2023-304
Preprint. Discussion started: 30 April 2024
© Author(s) 2024. CC BY 4.0 License.
Hydrology and Earth System Sciences Discussions
Open Access EGU

Met Eireann Report: *A summer of heatwaves and droughts*. Available at: https://www.met.ie/cms/assets/uploads/2018/09/summerfinal3.pdf [Accessed November 2019], 2018

Moore, P.: *Summer 2018*. Available at: https://www.met.ie/cms/assets/uploads/2020/06/Summer2018.pdf [Accessed February 2021], 2020

Murphy, R. M., Saunders, M., Richards, K. G., Krol, D. J., Gebremichael, A. W., Rambaud, J., Cowan, N., Lanigan, G. J.: Nitrous oxide emission factors from an intensively grazed temperate grassland: A comparison of cumulative emissions determined by eddy covariance and static chamber methods, *Agric. Ecosys. Environ.*, 324 107725, https://doi.org/10.1016/j.agee.2021.107725, 2022

Muñoz Sabater, J., Dutra, E., Agusti-Panareda, A., Albergel, C., Arduini, G., Balsamo, G., Boussetta, S., Choulga, M., Harrigan, S., Hersbach, H., Martens, B., Miralles, D. G., Piles, M., Rodriguez-Fernandez, N. J., Zsoter, E., Buontempo, C., Thepaut, J-N.: ERA5-Land: a state-of-the-art global reanalysis dataset for land applications, *Earth Sys. Sci. Data*, 13, 4349 - 4383, https://doi.org/10.5194/essd-13-4349-2021, 2021

Nie, W., Kumar, S. V., Arsenault, K. R., Peters-Lidard, C. D., Mladenova, I. E., Bergaoui, K., Hazra, A., Zaitchik, B. F., Mahanama, S. P., McDonnell, R., Mocko, D. M., and Navari, M.: Towards effective drought monitoring in the Middle East and North Africa (MENA) region: implications from assimilating leaf area index and soil moisture into the Noah-MP land surface model for Morocco, *Hydrol. Earth Syst. Sci.*, 26, 2365–2386, https://doi.org/10.5194/hess-26-2365-2022, 2022

Niu, G.-Y., Yang, Z.-L., Dickinson, R. E., Gulden, L. E., & Su, H.: Development of a simple groundwater model for use in climate models and evaluation with Gravity Recovery and Climate Experiment data. *Journal of Geophysical Research*, 112(D7), D07103. https://doi.org/10.1029/2006JD007522, 2007

Niu, G.-Y., Yang, Z.-L., Mitchell, K. E., Chen, F., Ek, M. B., Barlage, M., Kumar, A., Manning, K., Niyogi, D., Rosero, E., Tewari, M., and Xia, Y.: The community Noah land surface model with multiparameterization options (Noah-MP): 1. Model description and evaluation with local-scale measurements, *J. Geophys. Res.-Atmos.*, 116, D12110, https://doi.org/10.1029/2010JD015139, 2011

Noone, S., Broderick, C., Duffy, C., Matthews, T., Wilby, R.L. and Murphy, C.: A 250-year drought catalogue for the Island of Ireland (1765–2015). *International Journal of Climatology*, **37**(S1), 239–254, 2017

Or, D., and P. Lehmann: Surface evaporative capacitance: How soil type and rainfall characteristics affect global-scale surface evaporation. *Water Resour. Res.*, **55**, 519–539, https://doi.org/10.1029/2018WR024050, 2019

Paulik, C., Dorigo, W., Wagner, W., and Kidd, R.: Validation of the ASCAT Soil Water Index using in situ data from the International Soil Moisture Network, *Int. J. Appl. Earth Obs.*, 30, 1–8, https://doi.org/10.1016/j.jag.2014.01.007, 2014

Peel, M.C., Finlayson, B.L. and McMahon, T.A.: Updated world map of the Köppen–Geiger climate classification. *Hydrology and Earth System Sciences*, 11, 1633–1644, 2007

Poggio, L., de Sousa, L. M., Batjes, N. H., Heuvelink, G. B. M., Kempen, B., Ribeiro, E., and Rossiter, D.: SoilGrids 2.0: producing soil information for the globe with quantified spatial uncertainty, *SOIL*, 7, 217–240, 2021.

Sakaguchi, K., Zeng, X.: Effects of soil wetness, plant litter, and under-canopy atmospheric stability on ground evaporation in the Community Land Model (CLM3.5), *J. Geophys. Res.*,114, D01107, doi:10.1029/2008JD010834, 2009

Samaniego, L., S. Thober, R. Kumar, Wanders, N., Rakovec, O., Pan, M., Zink, M., Sheffield, J., Wood, E. F., Marx, A: Anthropogenic warming exacerbates European soil moisture droughts *Nat. Clim. Chang*., 8, 421-426, 10.1038/s41558-018-0138-5, 2018

Saxton, K. E., & Rawls, W. J.: Soil water characteristic estimates by texture and organic matter for hydrologic solutions. *Soil Science Society of America Journal*, **70**(5), 1569– 1578. https://doi.org/10.2136/sssaj2005.0117, 2006

Seneviratne, S.I., Corti, T., Davin, E.L., Hirschi, M., Jaeger, E.B., Lehner, I., Orlowsky, B. and Teuling, A.J.: Investigating soil moisture–climate interactions in a changing climate: a review. *Earth Science Reviews*, 99, 125–161, 2010.

Seneviratne, S.I. et al.: 'Changes in climate extremes and their impacts on the natural physical environment'. In: Managing the Risks of Extreme Events and Disasters to Advance Climate Change Adaptation [Field, C.B. et al. (eds.)]. Cambridge University Press, Cambridge, UK, and New York, NY, USA, 109-230, 2012 .

Shangguan, W., Y. Dai, Q. Duan, B. Liu, and H. Yuan, : A global soil data set for earth system modeling. *J. Adv. Model. Earth Syst.*, **6**, 249–263, https://doi.org/10.1002/2013MS000293, 2014

Skamarock, W. C., Klemp, J. B., Dudhia, J., Gill, D. O., Barker, D., Duda, M. G., … Powers, J. G.: *A Description of the Advanced Research WRF Version 3* (No. NCAR/TN-475+STR). University Corporation for Atmospheric Research, https://doi.org/10.5065/D68S4MVH, 2008

Svoboda, M., LeComte, D., Hayes, M., Heim, R., Gleason, K., Angel, J., Rippey, B., Tinker, R., Palecki, M., Stooksbury, D., Miskus, D., Stephens, S.: The Drought Monitor, *Bull. Amer. Meteor. Soc.*, 83, 1181 - 1190, https://doi.org/10.1175/1520-0477-83.8.1181, 2002

Szabó, B., G. Szatmári, K. Takács, A. Laborczi, A. Makó, K. Rajkai, and L. Pásztor, 2019. Mapping soil hydraulic properties using random-forest-based pedotransfer functions and geostatistics. *Hydrol. Earth Syst. Sci.*, **23**, 2615–2635, https://doi.org/10.5194/hess-23-2615-2019, 2019

Vereecken, H., Weynants, M., Javaux, M., Pachepsky, Y., Schaap, M. G., & van Genuchten, M. T.: Using pedotransfer functions to estimate the Van Genuchten-Mualem soil hydraulic properties—A review. *Vadose Zone Journal*, **9**, 795– 820. https://doi.org/10.2136/vzj2010.0045, 2010

Wagner, W., Lemoine, G., and Rott, H.: A method for estimating soil moisture from ERS scatterometer and soil data, *Remote Sens. Environ*., 70, 191–207, 1999.

Walsh S.: A summary of climate averages for Ireland, 1981 – 2010. MET Eireann CLIMATOLOGICAL NOTE No. 14, Dublin. https://www.met.ie/climate-ireland/SummaryClimAvgs.pdf , last accessed Oct., 2023, 2012

Warrach-Sagi, K., Ingwersen, J., Schwitalla, T., Troost, C., Aurbacher, J., Jach, L., et al.: Noah-MP with the generic crop growth model Gecros in the WRF model: Effects of dynamic crop growth on land-atmosphere interaction. *Journal of Geophysical Research: Atmospheres*, 127, e2022JD036518. https://doi.org/10.1029/2022JD036518, 2022

Weihermüller, L., P. Lehmann, M. Herbst, M. Rahmati, A. Verhoef, D. Or, D. Jacques, and H. Vereecken: Choice of pedotransfer functions matters when simulating soil water balance fluxes. *J. Adv. Model. Earth Syst.*, **13**, e2020MS002404M, https://doi.org/10.1029/2020MS002404, 2021

Xia, Y., Ek, M. B., Peters-Lidard, C. D., Mocko, D., Svoboda, M., Sheffield, J., Wood, E. F.: Application of USDM statistics in NLDAS-2: Optimal blended NLDAS drought index over the

© Author(s) 2024. CC BY 4.0 License.

continental United States, *JGR-Atmospheres*, 119, 2947-2965, https://doi.org/10.1002/2013JD020994, 2014

Xu, C., Torres-Rojas, L., Vergopolan, N., Chaney, N. W.: The benefits of using state-of-the-art digital soil properties maps to improve the modeling of soil moisture in land surface models, *Water Resour. Res.*, 59, e2022WR032336, https://doi.org/10.1029/2022WR032336, 2023

Zhang, Y., M. G. Schaap, and Y. Zha: A high-resolution global map of soil hydraulic properties produced by a hierarchical parameterization of a physically based water retention model. *Water Resour. Res.*, **54**, 9774–9790, https://doi.org/10.1029/2018WR023539, 2018

Zhang, Z., Laux, P., Baade, J., Arnault, J., Wei, J., wang, X., Liu, Y., Schmullius, C., Kuntsmann, H: Impact of alternative soil data sources on the uncertainties in simulated land-atmosphere interactions, *Agric. Fores. Meteor.*, 339, 109565, https://doi.org/10.1016/j.agrformet.2023.109565, 2023

Zhuo, L., Dai, Q., Han, D., Chen, N., Zhao, B.: Assessment of simulated soil moisture from WRF NOAH, NOAH-MP, and CLM land surface schemes for landslides hazard application, *Hydrol. Earth Sys Sci.*, 23, 4199-4218, https://doi.org/10.5194/hess-23-4199-2019, 2019

https://doi.org/10.5194/hess-2023-304
Preprint. Discussion started: 30 April 2024
© Author(s) 2024. CC BY 4.0 License.

Table 1. Summary of locations of in situ measurements. The station land cover and elevation data are obtained from Met Eireann service. The station soil texture data for Johnstown Castle and Dripsey are obtained from previous work (Kiely et al., 2018; Murphy et al., 2022), and soil texture map from the Irish Soil Information System (Creamer et al., 2014) are used for the in situ Terrain-AI sites

Sites	Lon/Lat (°)	Elevation (m)	Field Capacity	Soil texture category		
				In-situ	STATSGO	SOILGRIDS
Athenry	-8.786/ 53.2892	40.0	-	Loam	Loam	Loam
Ballyhaise	-7.309/ 54.0513	78.0	-	Loam	Clay-Loam	Loam
Claremorris	-8.992/ 53.7108	68.0	-	Sandy-Loam	Loam	Loam
Dunsany	-6.660/ 53.5158	83.0	-	Loam	Loam	Loam
Valentia	-10.244/ 51.9397	25.0	-	Sandy-Loam	Sandy-Loam	Loam
Johnstown Castle	-6.505/ 52.2981	52.0	0.32	Sandy-Loam	Loam	Loam
Dripsey	-8.752/ 51.9867	190.0	0.42	Loam	Loam	Loam

Table 2. Percentage proportion of grids covered by soil texture categories for STATSGO and SOILGRIDS databases used.

Soil texture	STATSGO (%)	SOILGRIDS (%)
Sandy Loam	16.4	27.0
Loam	57.8	71.5
Sandy Clay Loam	0	1.4
Clay Loam	19.5	0.1
Clay	6.3	0

© Author(s) 2024. CC BY 4.0 License.

Table 3. Summary of NOAH-MP physical options used in this study

Physical processes	Options
Vegetation	(4) Prescribed LAI + Prescribed max FVEG
Canopy stomatal resistance	(1) Ball-berry
	(2) Jarvis
Soil moisture factor	(1) Noah
Runoff and groundwater	(3) Noah (free drainage)
Surface layer drag	(1) Monin-Obukhov
Radiation transfer	(3) Gap=1-FVEG
Snow surface albedo	(2) CLASS
Precipitation partition	(1) Jordan (1991)
Lower boundary soil temperature	(2) Soil temperature at 8m depth
Snow/soil temperature time	(1) Semi-imiplicit
Surface resistance	(1) Sakaguchi and Zeng (2009)
Soil data	(1) Dominant soil texture
	(3) Soil composition and PedoTransfers
PedoTransfers	(1) Saxton and Rawls (2006)

Table 4. Definitions of drought categories based on Relative Soil Moisture (RSM) percentiles

ID	RSM percentile	Descriptions
Dryness		
D0	≤ 30	Abnormal
D1	≤ 20	Moderate
D2	≤ 10	Severe
D3	≤ 5	Extreme
D4	≤ 2	Exceptional
Wetness		
W0	≥ 70	Abnormal
W1	≥ 80	Moderate
W2	≥ 90	Severe
W3	≥ 95	Extreme
W4	≥ 98	Exceptional

https://doi.org/10.5194/hess-2023-304
Preprint. Discussion started: 30 April 2024
© Author(s) 2024. CC BY 4.0 License.

Table 5. Performance statistics of Relative Soil Moisture (RSM) for various soil texture categories at the topsoil (0 – 10 cm) and subsurface (0 – 100 cm) in STATSGO and SOILGRIDS for 2018 year. The errors are the median grid values. SL- Sandy Loam, L – Loam, SCL – Sandy Clay Loam, CL – Clay Loam, C – Clay.

Soil	RMSD		PBIAS		R	
texture	STATSGO	SOILGRIDS	STATSGO	SOILGRIDS	STATSGO	SOILGRIDS
Surface						
SL	0.016	0.016	-3.0	5.3	0.82	0.80
L	0.018	0.018	-7.8	-4.5	0.84	0.84
SCL	-	0.017	-	-6.0	-	0.84
CL	0.016	0.016	11.0	4.6	0.79	0.86
C	0.017	-	9.7	-	0.82	-
Subsurface						
SL	0.016	0.015	2.9	3.6	0.56	0.61
L	0.016	0.015	-1.9	-0.5	0.57	0.59
SCL	-	0.015	-	2.0	-	0.62
CL	0.014	0.015	4.5	-3.3	0.62	0.58
C	0.014	-	-1.3	-	0.61	-

Table 6. Performance statistics of Relative Soil Moisture (RSM) for various soil texture categories at the topsoil (0 – 10 cm) and subsurface (0 – 100 cm) in STATSGO and SOILGRIDS for 2019 year. The errors are the median grid values. SL- Sandy Loam, L – Loam, SCL – Sandy Clay Loam, CL – Clay Loam, C – Clay.

Soil	RMSD		PBIAS		R	
texture	STATSGO	SOILGRIDS	STATSGO	SOILGRIDS	STATSGO	SOILGRIDS
Surface						
SL	0.015	0.016	3.6	9.8	0.68	0.66
L	0.016	0.016	1.2	5.2	0.72	0.71
SCL	-	0.016	-	4.8	-	0.67
CL	0.019	0.018	21.2	18.0	0.61	0.81
C	0.019	-	20.1	-	0.79	-
Subsurface						
SL	0.013	0.012	17.8	16.7	0.61	0.63
L	0.011	0.012	13.8	16.4	0.68	0.71
SCL	-	0.013	-	19.1	-	0.73
CL	0.013	0.011	20.5	16.1	0.73	0.76
C	0.012	-	16.1	-	0.77	-

© Author(s) 2024. CC BY 4.0 License.

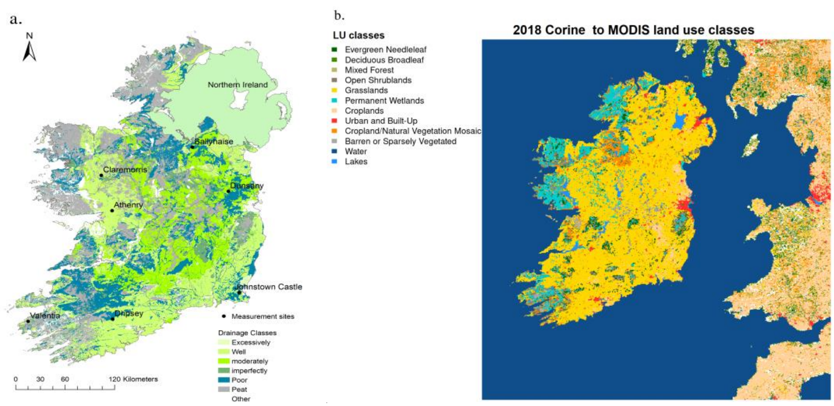

Figure 1. [a] Geographical locations of the selected in situ grassland sites overlaid on Ireland's map of soil drainage categories. [b] Refined map of 2018 Corine to MODIS land cover classes for the study domain.

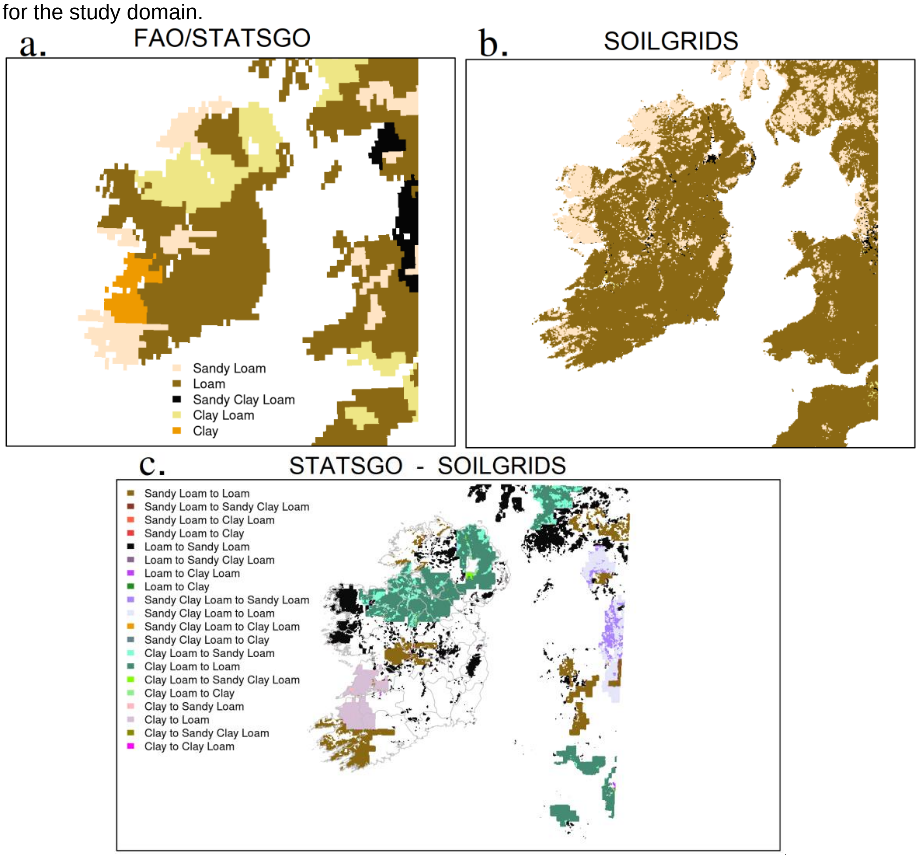

Figure 2. [a-b] Soil textural classes for the study domain based on global soil databases, namely FAO/STATSGO and SOILGRIDS. [c] Spatial differences in the soil texture categories between STATSGO and SOILGRIDS, indicating increasing or decreasing soil grain size.

Hydrology and Earth System Sciences
Open Access
Discussions

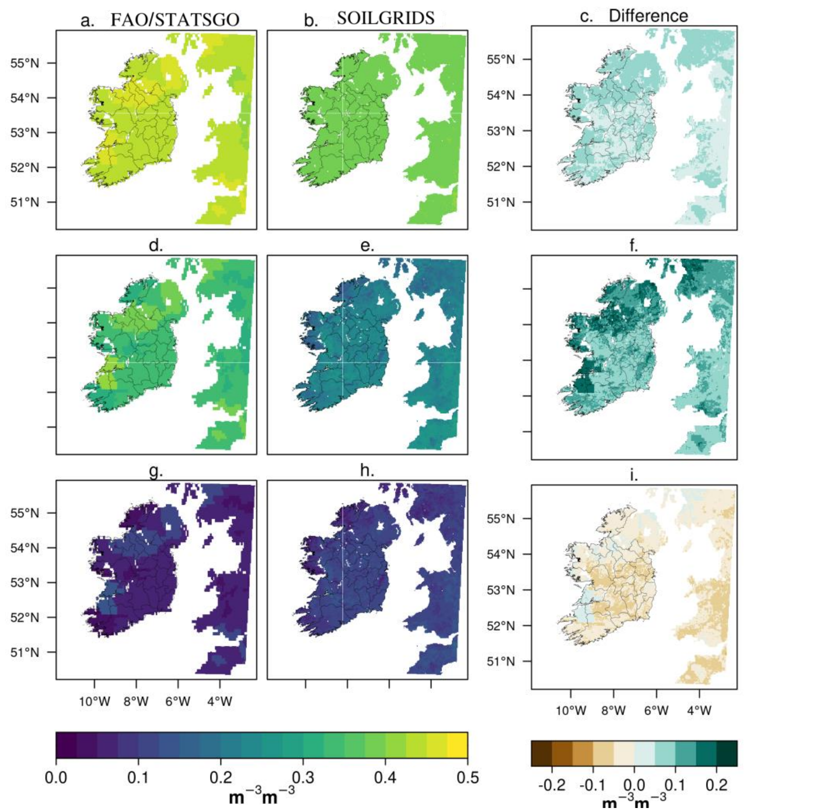

Figure 3. Spatial characteristics of absolute and difference between STATSGO and SOILGRIDS for [a-c] soil porosity, [d-f] field capacity and [g-i] wilting point.

https://doi.org/10.5194/hess-2023-304
Preprint. Discussion started: 30 April 2024
© Author(s) 2024. CC BY 4.0 License.

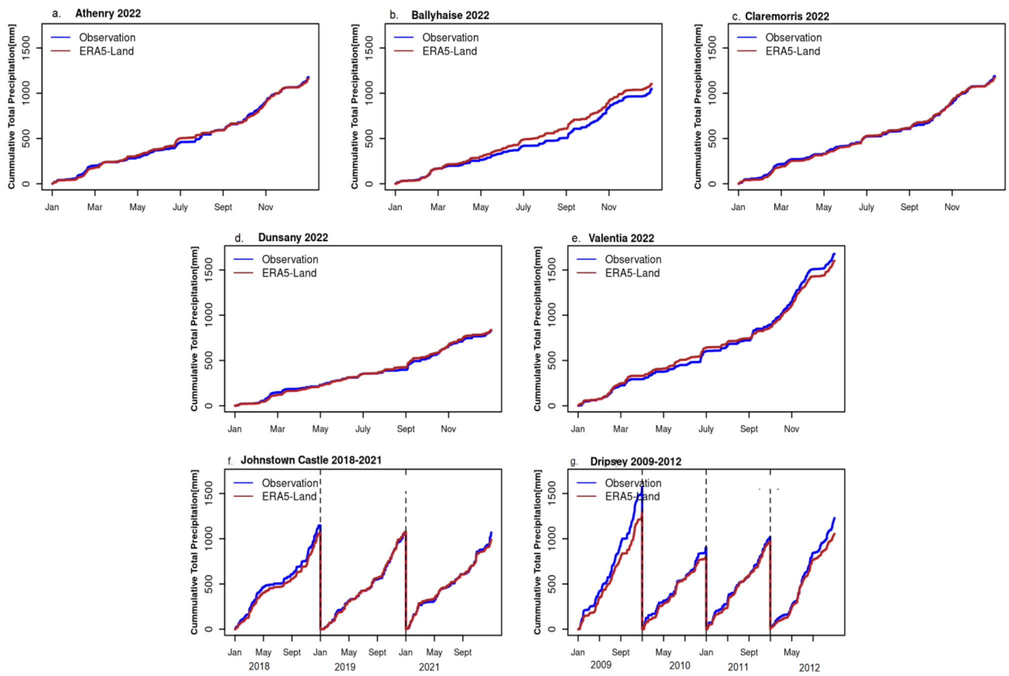

Figure 4. Temporal comparisons of observed total annual cumulative precipitation at the selected reference stations, against the ERA5-Land colocated grids.

https://doi.org/10.5194/hess-2023-304
Preprint. Discussion started: 30 April 2024
© Author(s) 2024. CC BY 4.0 License.
Hydrology and Earth System Sciences Discussions
Open Access
EGU

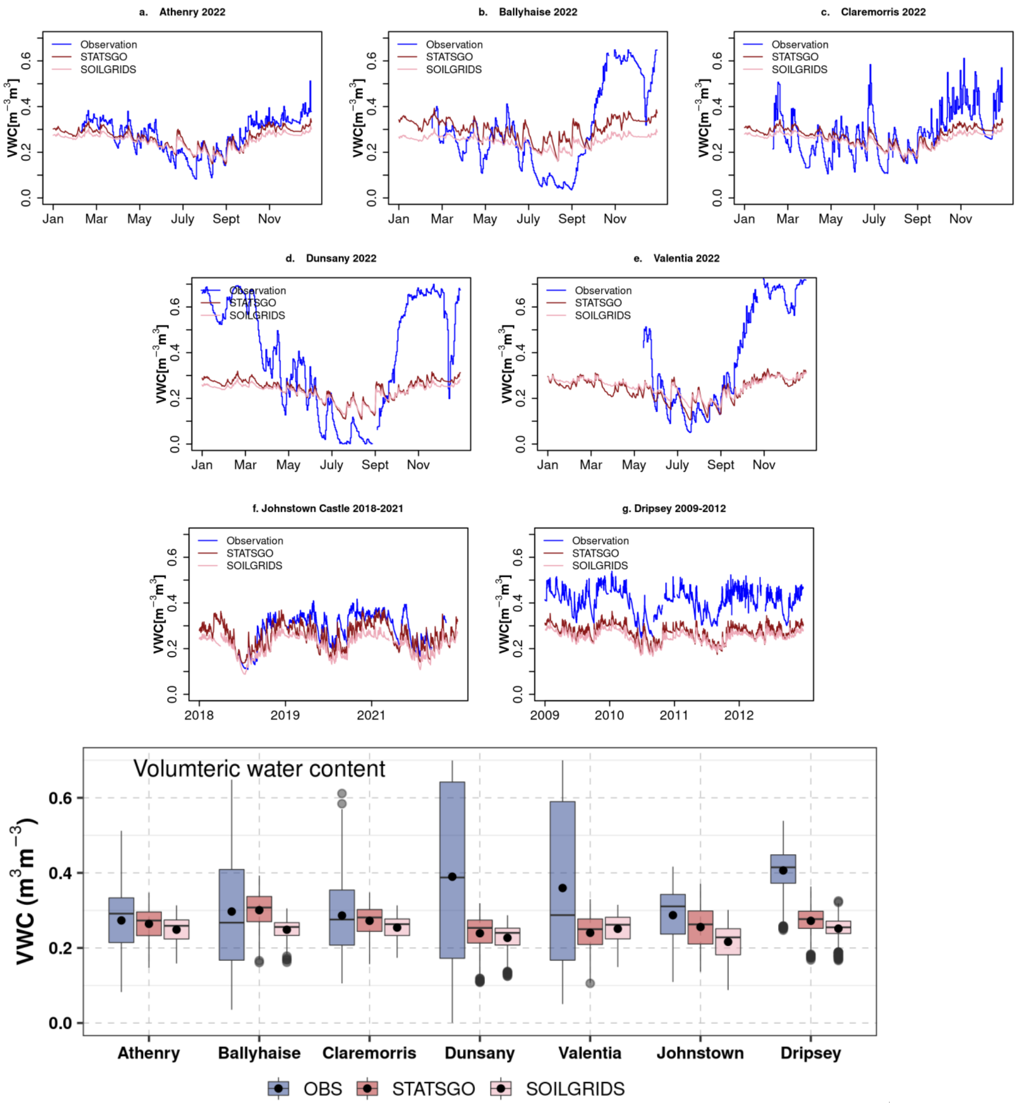

Figure 5. [a-g] Temporal comparisons of volumetric water contents and boxplots of data distribution, between observations and simulated values for the selected reference stations. The black dots in the boxes represent the mean values

https://doi.org/10.5194/hess-2023-304
Preprint. Discussion started: 30 April 2024
© Author(s) 2024. CC BY 4.0 License.
Hydrology and Earth System Sciences
Open Access
Discussions

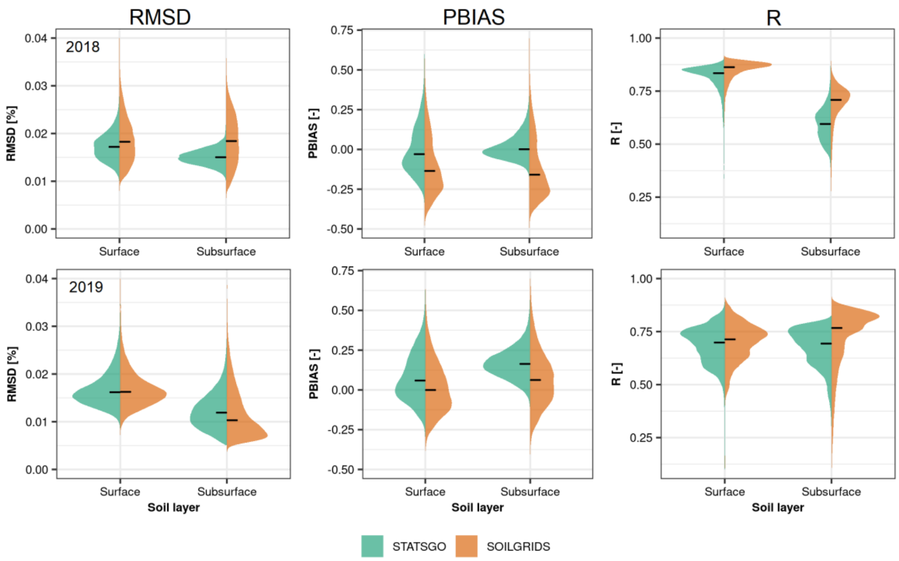

Figure 6. Performance statistics for STATSGO and SOILGRIDS derived Relative Soil Moisture (RSM) values at the topsoil layer (0-7 cm) and subsurface soil layer (0-100 cm), against satellite-based ASCAT Soil Water Index (SWI), for 2018 (top) and 2019 (bottom) years. N = 131,000 cells and the black crossbars are the median values.

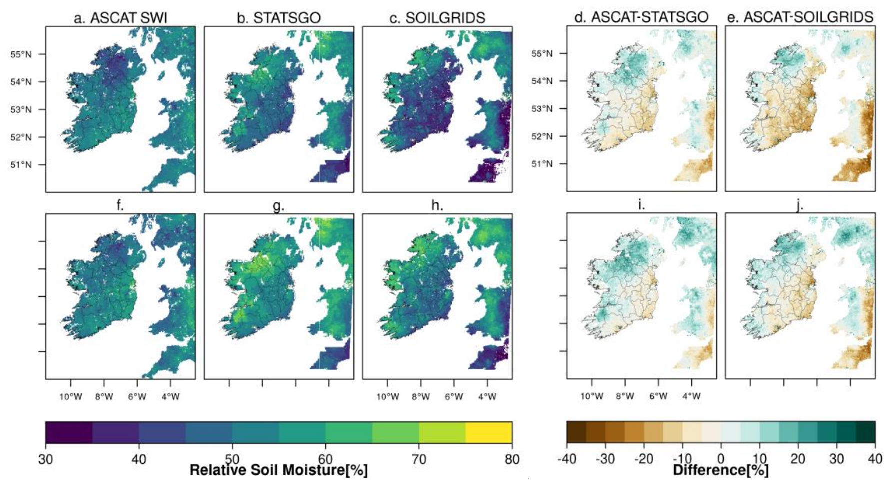

Figure 7. Spatial characteristics of absolute and difference between satellite-based annual ASCAT Soil Water Index (SWI) and model derived annual mean Relative Soil Moisture (RSM) at the surface , for [a-e] 2018 and [f-j] 2019 years

https://doi.org/10.5194/hess-2023-304
Preprint. Discussion started: 30 April 2024
© Author(s) 2024. CC BY 4.0 License.

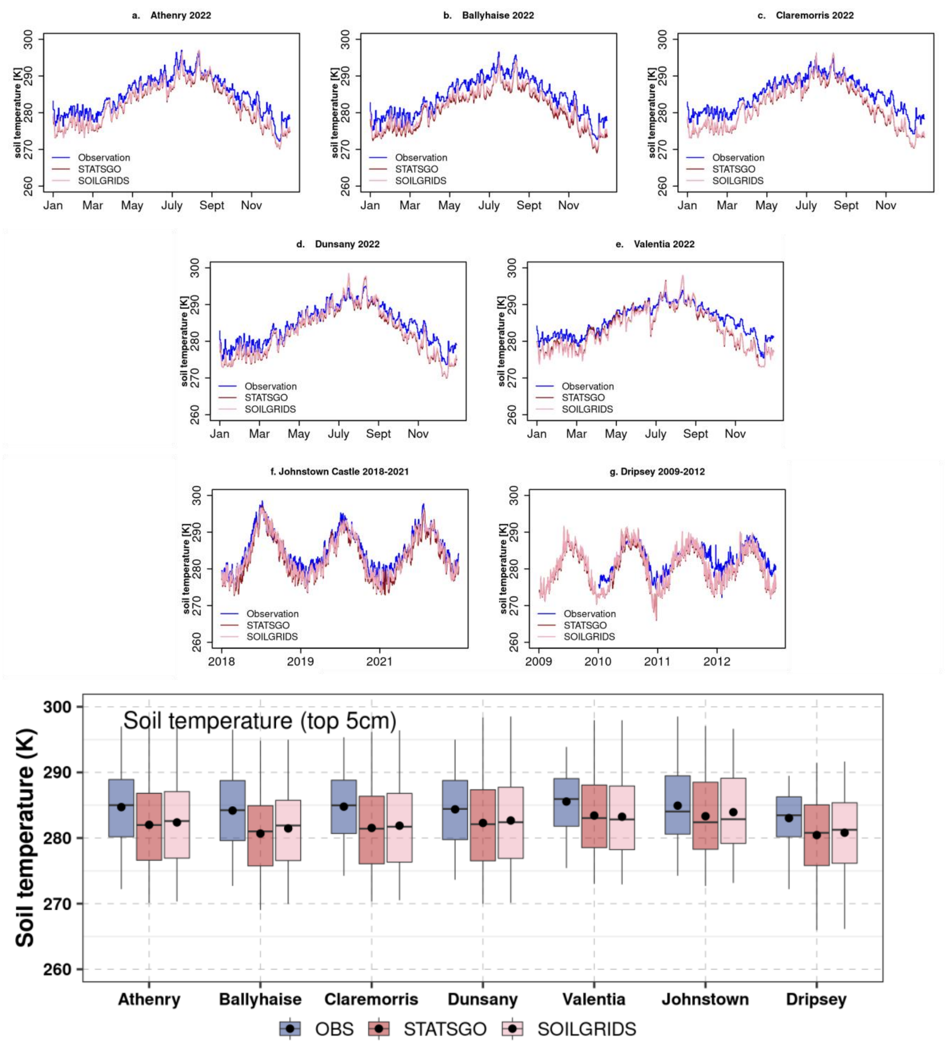

Figure 8. [a-g] Temporal comparisons of soil temperature and boxplots of data distribution, between observations and simulated values for the selected reference stations. The black dots in the boxes represent the mean values

https://doi.org/10.5194/hess-2023-304
Preprint. Discussion started: 30 April 2024
© Author(s) 2024. CC BY 4.0 License.
Hydrology and Earth System Sciences
Open Access
Discussions

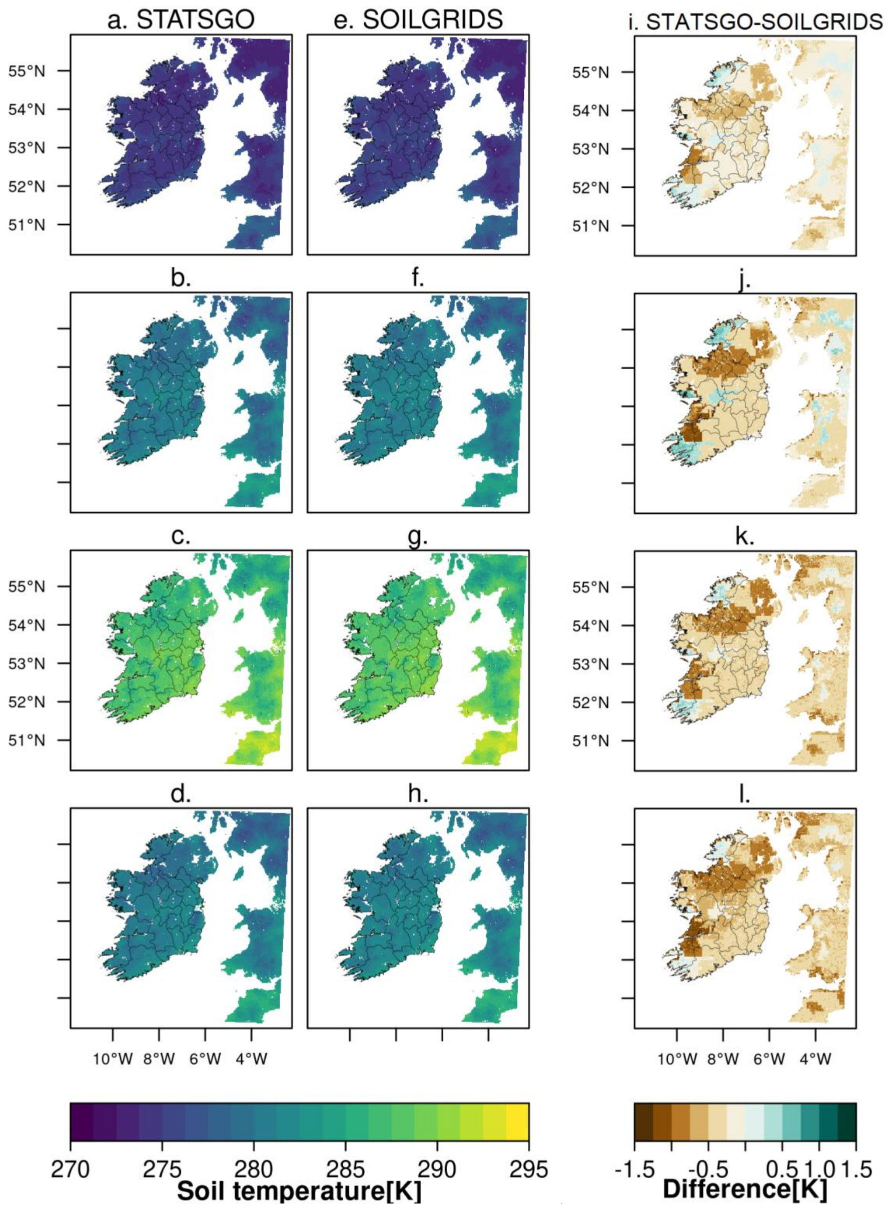

Figure 9. Spatial and seasonal characteristics of simulated top (0-7 cm) soil temperature using STATSGO [a-d], SOILGRIDS [e-h] and the difference [i-l], for the period 2009 - 2022. Rows [1-4] represent the Winter to Autumn seasons in that order.

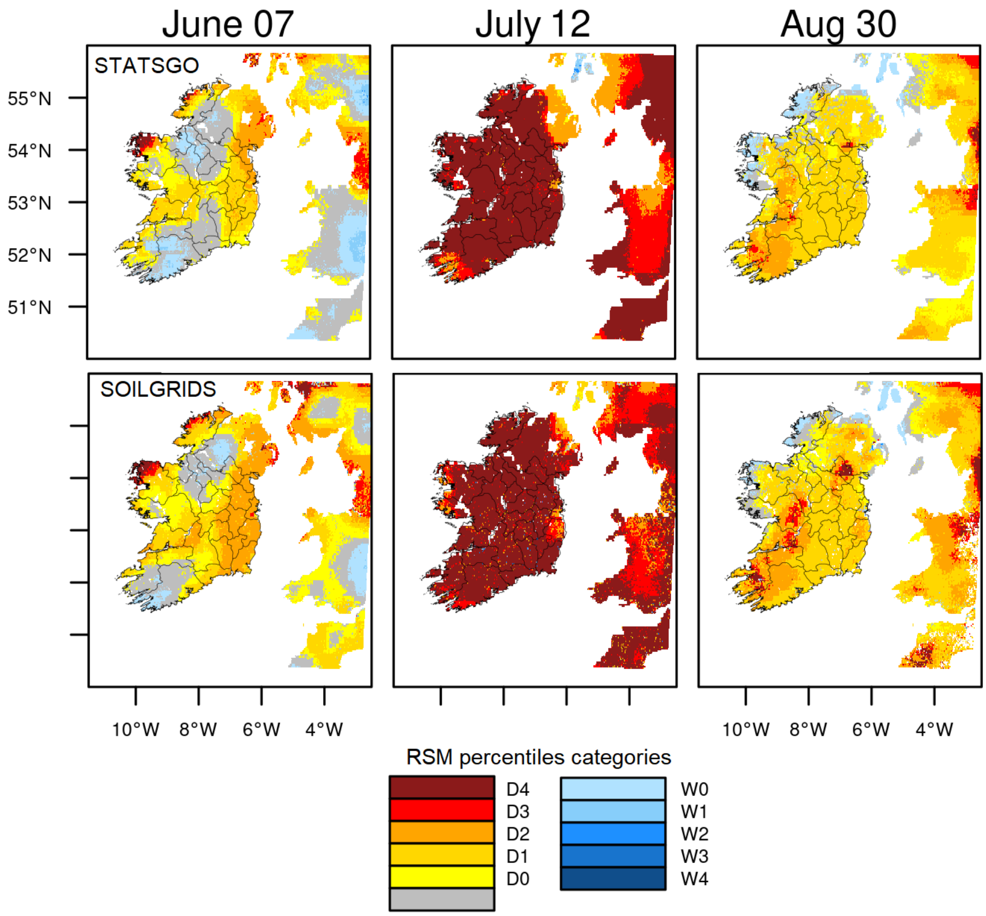

Figure 10. Spatial characteristics of soil moisture drought categories derived using 0 – 100 cm Relative Soil Moisture percentiles for STATSGO [top] and SOILGRIDS [bottom] for 2018 summer. D0-D4 represents abnormally dry, moderate, severe, extreme and exceptional droughts, while W0-W4 is the corresponding wetness categories.

https://doi.org/10.5194/hess-2023-304
Preprint. Discussion started: 30 April 2024
© Author(s) 2024. CC BY 4.0 License.

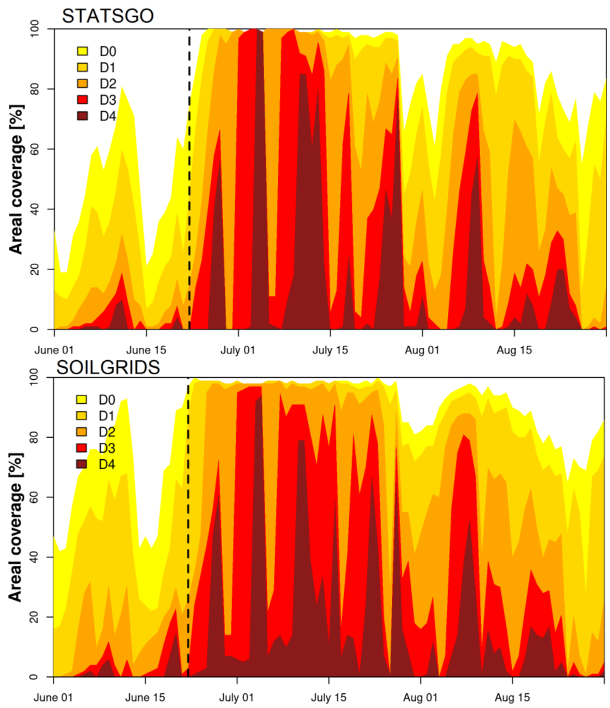

Figure 11. Time-areal coverage crossection of drought evolution based on daily 0 – 100 cm Relative Soil Moisture (RSM) percentiles during 2018 summer for STATSGO [top] and SOILGRIDS [bottom]. D0-D4 represents abnormally dry, moderate, severe, extreme and exceptional droughts. The dashed vertical lines represent the effective start of severe to exceptional droughts.

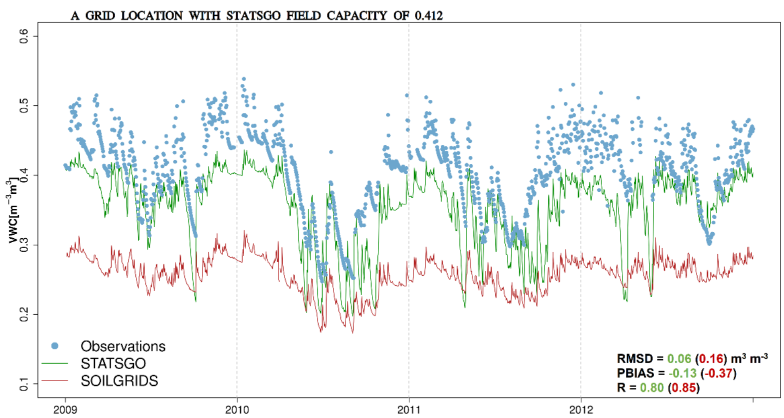

Figure 12. Temporal comparisons of observed volumetric water content (VWC) at Dripsey site, against the simulated values for a nearby grid location with field capacity of 0.412 $m^3 m^{-3}$.

Appendix

https://doi.org/10.5194/hess-2023-304
Preprint. Discussion started: 30 April 2024
© Author(s) 2024. CC BY 4.0 License.

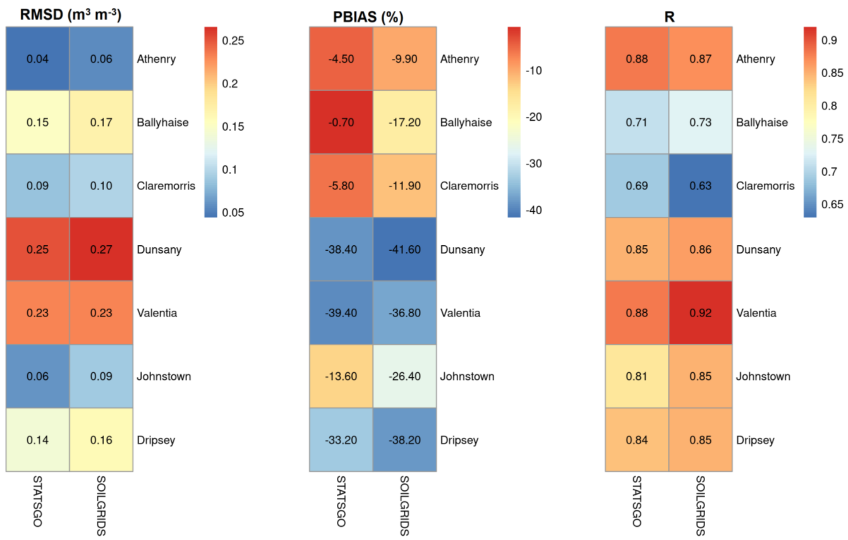

Figure A1. Error statistics of volumetric water contents between observations and model experiments for the selected reference stations.

© Author(s) 2024. CC BY 4.0 License.

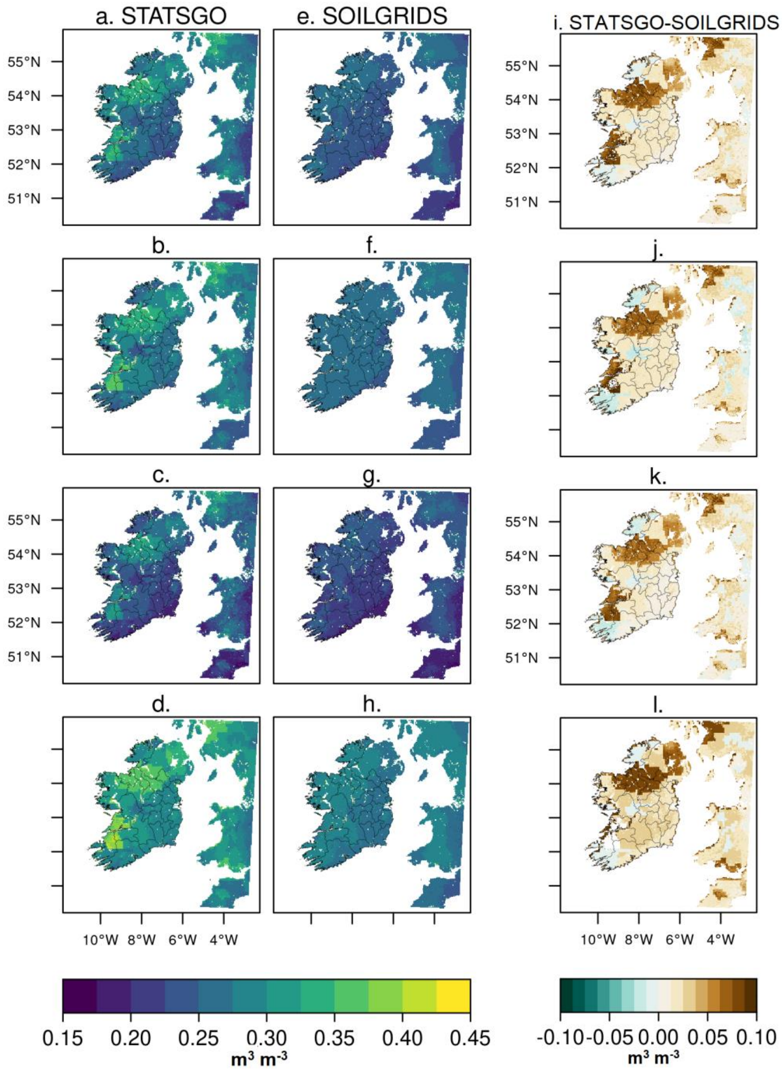

Figure A2. Spatial and seasonal characteristics of simulated top soil (0-7 cm) volumetric water content (VWC) using STATSGO [a-d], SOILGRIDS [e-h] and the difference [i-l], for the period 2009 - 2022. Rows [1-4] represent the Winter to Autumn seasons in that order

https://doi.org/10.5194/hess-2023-304
Preprint. Discussion started: 30 April 2024
© Author(s) 2024. CC BY 4.0 License.
Hydrology and Earth System Sciences
Open Access
EGU
Discussions

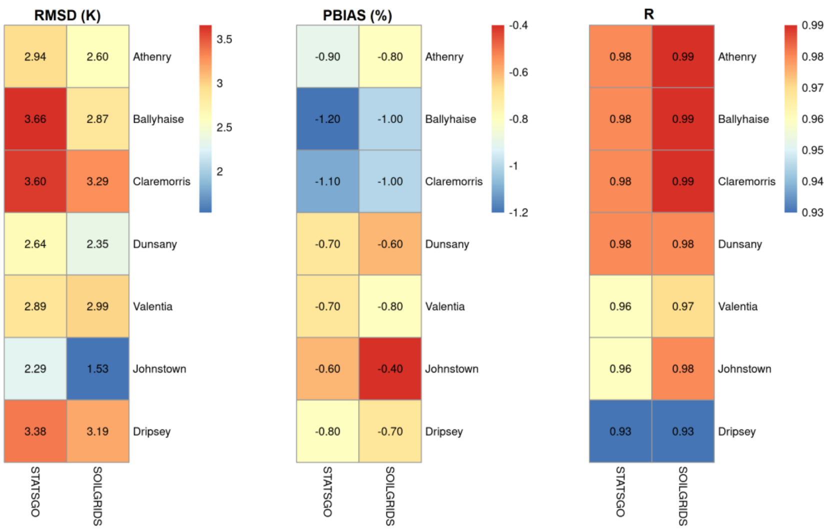

Figure A3. Error statistics of soil temperature between observations and model experiments for the selected reference stations.